Frequency Selective Surfaces: Design, Analysis, and Applications

Waseem Afzal [1,*], Muhammad Zeeshan Baig [2,*], Amir Ebrahimi [3], Md. Rokunuzzaman Robel [3], Muhammad Tausif Afzal Rana [4] and Wayne Rowe [3]

[1] Polytechnic Institute Australia (PIA), Melbourne 3003, Australia
[2] Wentworth Institute of Higher Education, Sydney 2010, Australia
[3] School of Engineering, RMIT University, Melbourne 3000, Australia
[4] King's Own Institute, Sydney 2000, Australia
[*] Correspondence: waseem@pia.edu.au (W.A.); muhammad.baig@win.edu.au (M.Z.B.)

Abstract: This paper aims to provide a general review of the fundamental ideas, varieties, methods, and experimental research of the most advanced frequency selective surfaces available today. Frequency-selective surfaces are periodic structures engineered to work as spatial filters in interaction with electromagnetic (EM) waves with different frequencies, polarization, and incident angles in a desired and controlled way. They are usually made of periodic elements with dimensions less than the operational wavelength. The primary issue examined is the need for more efficient, compact, and adaptable electromagnetic filtering solutions. The research method involved a comprehensive review of recent advancements in FSS design, focusing on structural diversity, miniaturization, multiband operations, and the integration of active components for tunability and reconfigurability. Key findings include the development of highly selective miniaturized FSSs, innovative applications on flexible and textile substrates, and the exploration of FSSs for liquid and strain sensing. The conclusions emphasize the significant potential of FSS technology to enhance wireless communication, environmental monitoring, and defense applications. This study provides valuable insights into the design and application of FSSs, aiming to guide future research and development in this dynamic field.

Keywords: frequency selective surfaces; spatial filters; periodic structures; electromagnetic waves

1. Introduction

Generally, FSSs are planar structures composed of a single or multiple stacked periodic metallic layers each printed on a dielectric substrate. In the design and realization of FSSs, various types of unit cells with diverse geometrical shapes can be used, such as patches [1–4], cross dipole [1], loops [5,6], hexagon [7,8], convoluted shapes [9,10], and fractal geometries. These elements produce frequency responses that are determined by the geometry of the structure within a period called a unit cell. However, depending on the material, geometry, and construction, the frequency responses of the filtering FSSs are divided into the 4 main categories of low pass, high pass, band stop, and band pass filters. FSSs can be designed with a broad range of functionalities in interaction with the incident electromagnetic waves. Figure 1 shows some distinguishable characteristics of wave interaction with FSSs.

Recent advancements in FSS research have concentrated on improving selectivity and miniaturization. Studies have explored innovative designs like dual-band miniaturized FSSs with high selectivity, providing efficient filtering of electromagnetic waves in multiple frequency bands [11]. Additionally, miniaturized multiband FSSs with wide frequency ratios have been developed, demonstrating the ability to operate across various frequency ranges while maintaining compact dimensions [12]. These innovations highlight the continuous evolution of FSS technology to meet the demands of modern wireless communication systems and electromagnetic interference mitigation strategies [13].
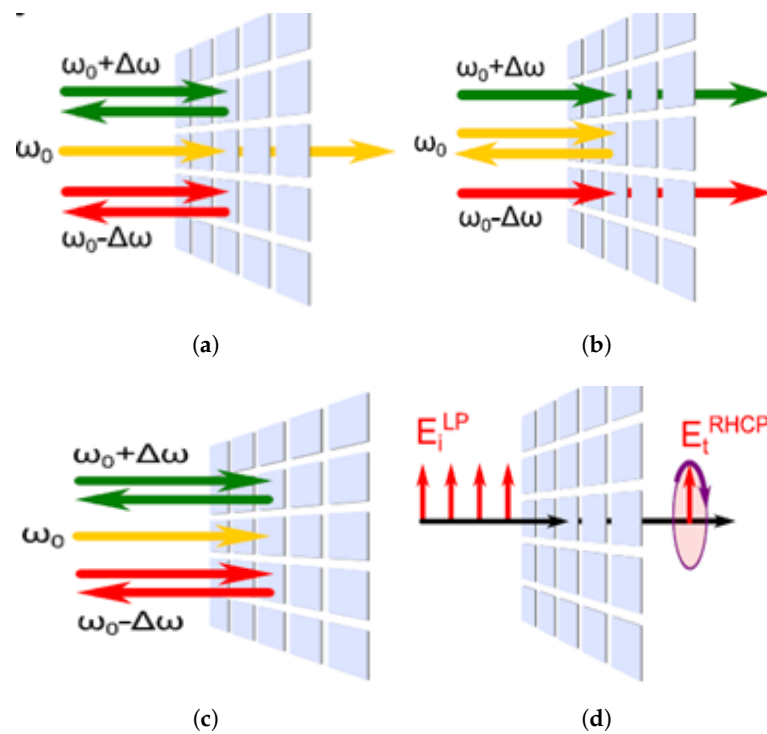
Figure 1. Wave interaction with FSS characteristics: (**a**) bandpass, (**b**) bandstop, (**c**) absorber, (**d**) polarization converter [14].

Researchers have also investigated incorporating active components into FSS designs to enable tunability and reconfigurability. Active FSSs with convoluted elements have been suggested for Ultra-High Frequency (UHF) applications, showcasing the potential for dynamic control over the surface's frequency response [15]. Moreover, studies on switchable and frequency-tunable active FSSs have shown promise in achieving versatile electromagnetic modulation capabilities, allowing for independent adjustments of frequency and amplitude responses [16]. These developments pave the way for adaptive FSS solutions that can cater to diverse operational requirements in communication and sensing systems.

In addition to traditional rigid substrates, the impact of flexible and textile substrates on FSS performance has been explored. Investigations into FSSs on flexible substrates have revealed the potential for conformal applications, enabling the development of highly efficient and miniaturized shields for electromagnetic compatibility in X-band frequencies [17]. Furthermore, studies on paper-based FSS designs utilizing slotlines have demonstrated the feasibility of implementing FSS technology on unconventional substrates, opening up possibilities for cost-effective and environmentally friendly electromagnetic filters [18].

The versatility of FSSs extends beyond conventional electromagnetic applications, with emerging research focusing on innovative functionalities. For instance, liquid sensors based on FSS principles have been proposed, showcasing the adaptability of these surfaces for sensing applications by modifying electromagnetic signals based on intrinsic resonant frequencies [19]. Moreover, popup tunable FSSs have been investigated for strain sensing, highlighting the potential for integrating FSS technology into structural engineering for diverse sensing and monitoring applications [20].

Recent studies have explored the development of high-performance frequency selective surfaces (FSSs) with advanced characteristics. Notably, high-temperature-resistant FSS metasurfaces have been designed to exhibit low backward scattering at lower frequencies and efficient transmission at higher frequencies, making them suitable for applications that require robust performance under extreme environmental conditions [21]. These advancements are critical for applications such as radar cross-section reduction and stealth technology, where maintaining performance under varying conditions is paramount [22].

Additionally, optically transparent dual-band FSSs have been proposed for smart surfaces, which are particularly relevant for Internet of Things (IoT) devices that necessitate specific design considerations related to transparency and dual-band functionality [23]. The integration of materials such as indium tin oxide and polyethylene terephthalate in the design of these transparent FSSs enhances their applicability in modern communication systems [24].

The latest research on frequency selective surfaces demonstrates various advancements aimed at enhancing selectivity, miniaturization, tunability, and functionality. These developments underscore the continuous innovation in FSS technology to address evolving requirements in wireless communication, sensing, electromagnetic compatibility, and structural engineering applications. The exploration of reconfigurable FSSs, which can adapt their characteristics through the use of active semiconductor devices, further exemplifies the trend towards dynamic and versatile applications in this field [25]. Moreover, the miniaturization of FSS designs, such as those employing convoluted structures, has proven essential for meeting the demands of modern communication systems, particularly in the millimeter-wave and terahertz frequency ranges [26]. These innovations collectively highlight the significant role of FSS technology in shaping the future of electromagnetic applications [27].

2. Applications of FSSs

FSSs have found a wide variety of applications, but conventionally, they have been used in radomes, multi-frequency reflector antennas, electromagnetic absorbers, polarization converters, etc. As shown in Figure 2 in a radome scenario, the FSS is employed to reduce the radar cross-section of the antennas, and it is transparent to a desired frequency band and reflective at other frequencies. An example of such an application is in aircraft, where a bandpass radome covers the antenna that is fixed at the tip. Radomes can be used in two ways in this situation: transparent mode and reflecting mode [28].

Figure 2. Radomes at the Cryptologic Operations Center, Misawa, Japan (photo courtesy of en. Wikipedia).

FSSs have also been used in multiband reflector antenna applications [29–32]. In such applications, the FSS is used as a sub-reflector, where it is designed to be reflective at a frequency band and simultaneously transparent at other bands. Hence, the sub-reflector allows for the application of multiple feeds and enables the multiple frequency state antennas. Different frequency feeds are positioned at real centers of the sub-reflector, and the single reflector geometry acts as a multiband antenna. A practical example is the high-gain antenna of the Voyager spacecraft that was designed in [29], where the FSS forms the sub-reflector that reflects at X-band and transmits the S-band as shown in Figure 3. In this antenna, the S-band is placed at the focal point of the reflector, while the X-band is

located at the Cassegrain focal point. The single reflector architecture acts as a dual-band antenna reducing the mass, volume, and fabrication cost.
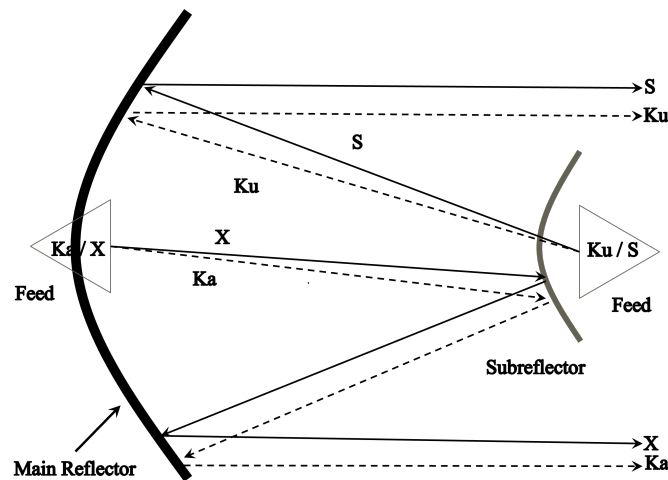

Figure 3. Cassini high-gain antenna (HGA) with a four-band FSS [2].

Figure 4 shows the construction of an *LC* resonating surface incorporating an array of metallic strips, which are truncated at specific intervals to form capacitive junctions. The metallic grids are inductive and in combination with the capacitive gaps form a series *LC* resonator. The frequency response of the array can be tuned by adding lumped elements like varactor diodes.
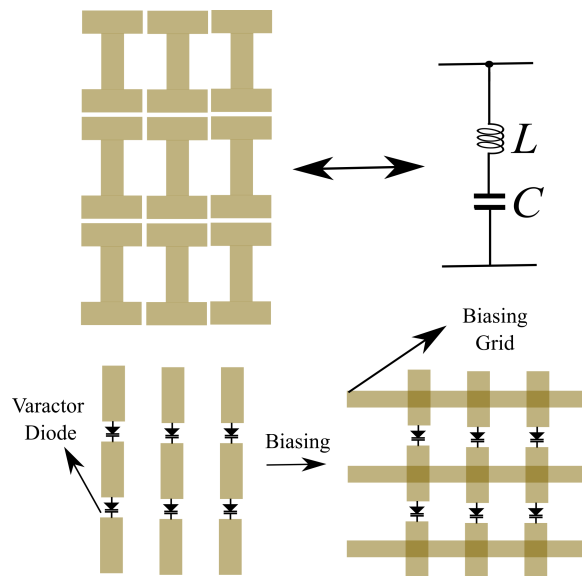

Figure 4. An active LC array comprising metallic strips interrupted by gaps in a periodic fashion. The gaps can be loaded with varactor diodes to alter the gap capacitance [5].

Recently, FSSs have been implemented using new materials such as conductive inks and transparent dielectric polymers. In such structures, the FSSs may be printed on walls and windows of libraries, prison cells, and theaters to block mobile phone signals, while simultaneously allowing emergency Terrestrial Trunked Radio (TETRA) services to operate. A simple FSS is used in the door of microwave oven and acts as a high-pass filter. The door blocks the 2.4 GHz microwaves inside and also allows the visible light to pass through the door. Table 1 presents typical applications of the FSS.

Table 1. Practical applications of FSSs.

FSS Refs.	Application	FSS Refs.	Application
[33–35]	MMs FSS	[36–38]	FSS for mobile communication
[39–41]	MM/MSs Lens	[33,42,43]	X band
[44–46]	Textile FSS	[47,48]	C band
[49–51]	Optical FSS/MSs	[52]	5G EMI reduction
[53]	Near Infrared	[34]	RCS reduction
[54,55]	Infrared	[56–58]	Secure wireless network
[59]	Filtering/Anti-reflecting coating	[60–64]	RF interference and harmonic suppression
[65–68]	Wearable FSS	[52,69–71]	EMI shielding
[72–75]	FSS absorber	[76]	Radio Astronomy
[77,78]	Sensors	[79]	Dichroic sub-reflector
[80–82]	RFID	[83,84]	Terahertz band
[82,85–88]	FSS antenna	[72,89–92]	Stealth radomes
[93]	Reconfigurable mechanisms	[94]	Wireless Charging

The functionality of an FSS is highly dependent on the unit cell size and geometry. Thus, appropriate modeling and synthesis procedures should be developed for the efficient design of FSSs for different applications. The following section covers the properties of FSSs, i.e., element shapes, standard responses, configurations, angular stability, unit cell size, and analysis methods.

2.1. Intelligent Reflecting Surfaces (IRSs)

Intelligent Reflecting Surfaces (IRSs) have become a transformative technology in modern wireless communication systems, particularly for their ability to manipulate electromagnetic (EM) waves in real-time. These surfaces consist of large arrays of low-cost reflecting elements, which can be either passive or active, and are placed strategically to improve signal quality and coverage [95].

Passive IRS utilizes reconfigurable, but non-powered, elements (e.g., metallic patches or dipoles) that reflect incoming signals based on their geometrical configuration and material properties. By adjusting the orientation and spatial configuration of these passive elements, signals can be directed toward specific areas, reducing the chances of coverage holes in areas traditionally plagued by poor reception (i.e., blind spots). This makes a passive IRS particularly effective in complex urban environments, where signals are often obstructed by buildings or other large structures [96].

Active IRS, on the other hand, integrates tunable components such as varactor diodes, PIN diodes, or even micro-electro-mechanical systems (MEMS), allowing for the surface to dynamically adjust the phase and amplitude of reflected signals. An active IRS provides enhanced control over the EM wave properties, enabling real-time adjustments to signal paths. These surfaces can actively suppress interference or nullify jamming attempts by fine-tuning the reflection coefficients of each element. The reconfigurable nature of an active IRS also allows for these surfaces to respond to changing environmental conditions, such as user movement or fluctuating interference patterns [97].

This combination of passive and active IRSs provides unprecedented flexibility and control in shaping wireless environments, ensuring more reliable communication even in the presence of obstacles or interference. IRS technology can be applied in various communication scenarios, including but not limited to cellular networks, satellite communications, and vehicular networks.

2.2. IRSs for Cellular Networks

One of the most critical applications of IRSs is within cellular networks, particularly in densely populated urban environments where buildings and other physical structures can obstruct signal propagation. An IRS has the unique ability to "reflect" and direct wireless signals into areas that would otherwise suffer from poor coverage. For example, an IRS placed on the exterior of a building can reflect signals from a base station to users located in areas where direct line-of-sight transmission is impossible, effectively solving the problem of blind spots [98].

2.2.1. Enhancing Secrecy Rates

In cellular communication systems, the security of transmitted data is paramount, especially in environments prone to eavesdropping or signal interception. An active IRS, with its ability to dynamically alter the reflection pattern, can be employed to enhance secrecy rates by directing signals away from potential eavesdroppers [99]. For instance, IRSs can leverage advanced beamforming techniques, where reflected signals are concentrated toward legitimate receivers while nullifying the signal in directions of potential eavesdroppers. By carefully adjusting the phase shifts of each IRS element, active surfaces can ensure that only the intended recipient receives the signal at full strength, while the signal remains weak or incoherent elsewhere.

2.2.2. Interference Mitigation

Cellular networks are often plagued by interference, particularly in densely populated areas where multiple users compete for a limited spectrum. IRSs can mitigate interference in two ways: first, a passive IRS can be strategically placed to reflect signals away from interference sources; second, an active IRS can dynamically adjust their configurations to either reflect interfering signals away from the receiver or cancel out the interference altogether through destructive interference techniques [100]. The surface achieves this by applying calculated phase shifts to incoming signals, ensuring that interfering signals are either redirected or canceled at the receiver's location [101].

2.2.3. Beamforming Integration

Beamforming technology is commonly used in modern communication systems to direct signals in specific directions, increasing efficiency and signal strength for targeted receivers. IRSs can complement this technology by acting as "smart reflectors" that enhance the beamforming capabilities of base stations. In this setup, the IRS elements adjust their reflection angles and phases to further direct the signal beams, improving communication quality even when users are in highly obstructed environments. This synergy between IRS and beamforming significantly enhances spectral efficiency and reduces energy consumption in the network [102].

2.2.4. Phase Shifts and Real-Time Adaptation

Another critical feature of IRS technology is its ability to introduce phase shifts to the reflected signals. By controlling the phase of each element in the array, IRSs can adjust the wavefront of the reflected signals, directing them toward the desired receiver with minimal loss. This allows for real-time adaptation to changes in the environment, such as user mobility and shifting interference patterns, ensuring that the communication link remains stable and secure [103].

The IRS is particularly advantageous for future communication systems, such as 5G and beyond, where the ability to control the wireless propagation environment will become increasingly important. The use of IRSs in these systems promises enhanced data rates, improved energy efficiency, and higher security, making it a critical component of next-generation wireless infrastructure.

2.3. FSS in Wireless Communications

Frequency selective surfaces (FSSs) are an effective tool in wireless communication systems for controlling the beamwidth and sidelobe levels of antenna arrays. By selectively filtering specific frequencies, FSSs improve the directionality and reduce unwanted radiations or side lobes that can cause interference in adjacent frequency bands.

2.3.1. Beamwidth Control

Beamwidth refers to the angular spread of the main lobe of an antenna radiation pattern. An FSS enhances beamwidth control by modifying the geometry and periodicity of the surface elements. Research has shown that by optimizing the shape and size of FSS elements (e.g., hexagonal, fractal, or cross-dipole geometries), the beamwidth can be reduced by 10–30%, which tightens the radiation pattern and improves signal directionality. For instance, using cross-dipole FSS structures can narrow the beamwidth from approximately 70° to 50° [104].

2.3.2. Sidelobe Level Reduction

Sidelobes represent unwanted radiation in directions other than the main lobe, which can lead to interference. FSS-based antennas effectively reduce sidelobe levels through the careful design of the unit cell structure and element distribution. By incorporating multi-layer FSSs with sub-wavelength elements, researchers have demonstrated sidelobe reduction by up to 20 dB, significantly minimizing interference from adjacent frequencies [105]. The reduction in sidelobe levels improves signal clarity and enhances spectral efficiency in crowded communication environments such as urban areas [106].

2.3.3. Enhancing Front-to-Back Gain

The front-to-back ratio (F/B) is the ratio of the power radiated in the forward direction (main lobe) to the power radiated in the opposite direction (back lobe). This metric is crucial for ensuring that most of the radiated power is concentrated in the desired direction, minimizing energy loss [107]. Using FSSs, particularly with multi-layer configurations, can substantially increase the front-to-back gain by manipulating the reflection and transmission properties of the surface elements [108].

For example, studies have shown that by utilizing multi-layer FSS with fractal and hexagonal elements, the front-to-back gain can be increased by up to 10 dB, enhancing the directivity and efficiency of the antenna [109]. This is achieved by carefully tuning the reflection phase of the FSS elements, which reduces back radiation and concentrates more power in the forward direction.

2.3.4. Bandwidth Expansion

Bandwidth refers to the range of frequencies over which the antenna maintains efficient performance. FSS elements can expand the bandwidth of antenna arrays by allowing for multiple frequency bands to pass through or be reflected, depending on their design. The use of multi-layer-FSSs, incorporating various unit cell geometries such as fractal, hexagonal, and Jerusalem cross, has been shown to increase the bandwidth by 20–40% compared to traditional antenna designs [104]. The bandwidth Δf of an FSS is defined as follows:

$$\Delta f = f_H - f_L \tag{1}$$

The fractional bandwidth can be expressed as follows:

$$\text{Fractional Bandwidth} = \frac{\Delta f}{f_0} = \frac{f_H - f_L}{f_0} \tag{2}$$

where

- f_H is the upper cutoff frequency.
- f_L is the lower cutoff frequency.

- f_0 is the center frequency.

2.4. Microwave and Millimeter-Wave Applications

In microwave and millimeter-wave applications, controlling reflection is essential for reducing interference and signal degradation. Reflection, if uncontrolled, can cause multipath effects, where the same signal arrives at the receiver from different paths, resulting in destructive interference and reduced signal quality.

FSSs can be designed to minimize reflection at specific frequency bands by carefully adjusting the periodicity and geometry of the elements (such as square patches, dipoles, and fractals). For instance, an FSS structure can be optimized to have a low reflection at 28 GHz (a common millimeter-wave band for 5G) by ensuring that the surface's elements resonate at this frequency, allowing for most of the signal to pass through the surface with minimal reflection.

Recent developments in FSS design have focused on creating wideband FSS structures that maintain low reflection and return loss across multiple frequency bands. These structures are particularly useful in applications like radar and satellite communications, where wideband performance is critical. For example, a novel concentric ring FSS design achieved a return loss of -25 dB across the 18 GHz to 40 GHz range, making it ideal for multiband communication systems [110].

A low return loss is also a hallmark of a well-designed FSS, particularly in systems operating in the microwave and millimeter-wave ranges. Return loss affects how much of the signal energy is reflected back toward the source. A high return loss, or poor transmission, leads to power loss and reduced efficiency, making the system less reliable. This is especially critical in wireless systems where signal strength and efficiency are paramount.

The reflection coefficient describes how much of the incident electromagnetic wave is reflected back by the surface. It is often used to assess how well the FSS rejects or transmits signals at specific frequencies.

$$S_{11} = 20 \log_{10}\left(\frac{V_{\text{reflected}}}{V_{\text{incident}}}\right) \tag{3}$$

where

- $V_{\text{reflected}}$ is the amplitude of the reflected wave.
- V_{incident} is the amplitude of the incident wave.

The transmission coefficient represents how much of the incident wave passes through the FSS. It is crucial for evaluating the filtering efficiency of the surface at different frequencies.

$$S_{21} = 20 \log_{10}\left(\frac{V_{\text{transmitted}}}{V_{\text{incident}}}\right) \tag{4}$$

where

- $V_{\text{transmitted}}$ is the amplitude of the transmitted wave.
- V_{incident} is the amplitude of the incident wave.

Return loss quantifies the power loss in the signal reflected back to the source and is closely related to the reflection coefficient S_{11}. A lower return loss indicates that most of the signal is transmitted through the FSS.

$$\text{Return Loss} = -20 \log_{10}(|S_{11}|) \tag{5}$$

For example, in satellite communications, a low return loss ensures that the signal transmitted from the ground station is efficiently directed toward the satellite with minimal loss. Similarly, in 5G systems, where millimeter-wave frequencies (e.g., 26 GHz, 28 GHz, 39 GHz) are used for high-data-rate transmissions, maintaining a low return loss allows for the system to provide a high throughput and stable connections over longer distances.

In recent studies, researchers have achieved significant reductions in return loss using FSSs in millimeter-wave applications. For instance, in a study focused on 5G antennas, a multi-layer FSS was employed to reduce return loss at 28 GHz by 30 dB, demonstrating highly efficient signal transmission across a wide frequency range [110].

3. Elements of Frequency Selective Surfaces

Frequency-selective surfaces can be broken down into three major configuration classification: namely, element-based FSSs, structure-based FSSs, and application-oriented, as shown in Figure 5. Traditionally, FSSs were made of resonant elements with dimensions comparable with the wavelength at the operational frequency. In such structures, an array of metallic elements is illuminated by a plane wave that stimulates the electric current on elements. The amplitude of the induced current depends on the strength of coupling between the elements and the wave, while the highest level of coupling occurs at the fundamental frequency, where the length of the element is $\lambda/2$. The frequency response of the FSS is determined by the distribution of the electric current on elements, dependent on the element's shapes. Since the resonance in traditional FSSs is dependent on the length of the unit cell, the excitation of higher-order resonance modes is unavoidable. As an indication, the current distribution along a single element of a resonant FSS is presented in Figure 6, showing the distribution of current for the fundamental resonance and its first harmonic. Some specific harmonics of FSSs are excited under oblique incidences. Thus, the frequency response might be highly degraded under oblique incidence.
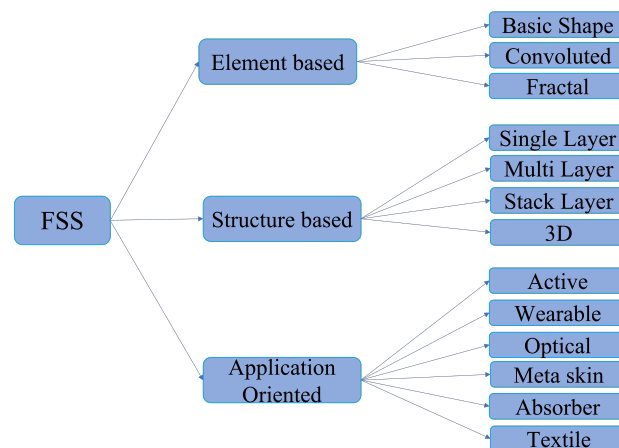

Figure 5. Classification of FSSs.
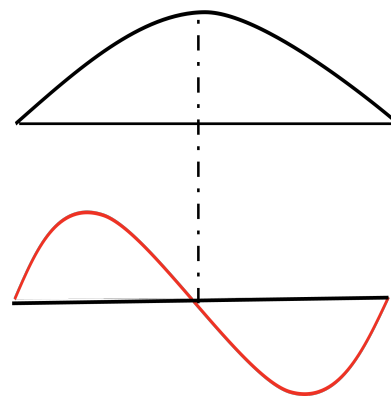

Figure 6. Current distribution at the first and the second resonant modes—(**top**) shows the fundamental mode (frequency f_0), which is excited for any element shape irrespective of the incidence angle; (**bottom**) shows the first odd mode at about $2f_0$, which may be excited at oblique incidence. The frequency of this mode may change slightly depending on the element shape [1].

Even though the geometry of elements has a major impact on filtering, other parameters such as the dielectric properties of the substrate supporting the elements and the spacing between them also influence the frequency of operation and the bandwidth. For a better understanding of the FSS operation, it is essential to understand the structure of FSSs. Here, we study the main unit cell geometries used in the design of traditional resonant FSSs [111]. The four major categories of the unit cells used in the traditional designs are as follows:

1. N-poles or center-connected, such as dipole, three-legged element or tri-poles, Jerusalem cross, cross dipoles, and the square spiral, as shown in Figure 7a.
2. Loop types, such as the three- and four-legged loaded elements, the circular loops or rings, square, and hexagonal loops, as shown in Figure 7b.
3. Solid interiors or plate types mainly in patch or aperture forms, i.e., square meshes and circular patches, as shown in Figure 7c.
4. Combinations or sophisticated patterns, i.e., combination of solid interior shapes or center-connected loops to overcome the deficiencies with simple shaped elements as shown in Figure 7d.

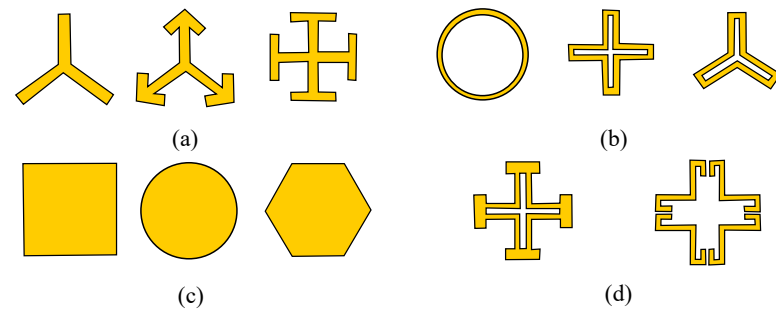The four groups of the unit cells are discussed in the following sub-sections.

Figure 7. Typical shapes of FSSs. (**a**) N-pole or center-connected; (**b**) Loop type; (**c**) Solid interiors; (**d**) Combination of either first three [112].

3.1. Class 1: N-Pole or Center-Connected Elements

The first group is represented by an array of tri-poles, where the elements consist of three concentric, thin monopoles that share a common center point. The tri-poles can be packed closely to reduce the spacing between elements, which enhances their bandwidth. The group also contains the Jerusalem cross, which is the oldest building block of FSSs. The Jerusalem cross comprises two crossing dipoles, which have small orthogonal sections at the ends. Also, the Jerusalem cross has superior stability as compared to the tri-pole; as in tri-poles, the angle of incidence changes both the bandwidth and harmonics [111].

3.2. Class 2: Loop Type

This group contains the closed loop elements, which are either simple or meandered to reduce the size. These elements are resonant when the total lengths of the metallic trace is equal to full wavelengths at the operation frequency. Transmission line theory explains the operations mechanism of the cross-shaped loop element. The half dipole arms are akin to a shorter dipole that is loaded with reactance. This class also has hexagonal elements that have better scan stability [111].

3.3. Class 3: Solid Interiors or Plate Type Elements

This group includes the plate type elements, which are of two types: (i) metallic patches mainly in shapes of a circular disk, rectangle, and square; (ii) an array of slots on metallic plates in shapes such as square, circular, etc., as shown in Figure 8. The first type is used as reflecting arrays while the other implements transparent arrays. As the patch dimensions of this group are close to $\lambda/2$, they suffer from the issue of angle dependence and the onset of grating lobes [111].
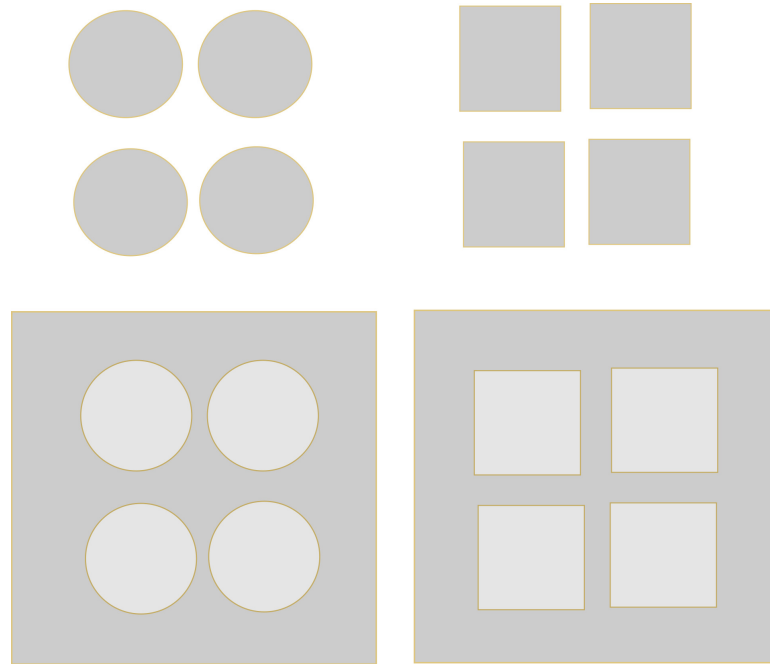
Figure 8. Examples of the third class of FSSs, the plate type elements [111].

3.4. Class 4: Combination Elements

This class consists of a broad range of elements because it represents combinations of the elements from the other three groups to construct new elements. The different shapes of elements enable the creation of diverse frequency responses [111].

3.5. Evaluation of the Four Classes of FSSs

When being used as the spatial filters, FSS structures should have low dependence on the angle of incidence to ensure operational performance. In order to make the resonance frequency of an FSS more stable with respect to variation of the incidence angle, generally, the inter-element spacing is reduced as compared with the wavelength. A higher level of grating lobes is created with large spacing, and the resonance frequency moves lower with the angle of incidence [111]. Among the mentioned classes of FSSs, group 2 (loop type) elements have a high angle stability. Although some of the elements of this class (three- and four-legged, square, and circular loops) may have different appearances, their operation can be related to dipoles, i.e., a square loop can be understood as two bent dipoles. Consequently, when the two dipoles are at resonance, the loop resonates. Therefore, the mentioned condition is satisfied when the circumference of the loop is one wavelength (λ). However, for better scan angle performance, they must be packed in a small area.

Table 2 lists the performance of FSSs with different element shapes mainly based on freestanding FSS performance [113]. Ratings: best = 1, second best = 2, third best = 3, least = 4. The performance is compared across 4 categories: Cross Polarization, Stability, Band Separation, and Larger Bandwidth. Each shape—Jerusalem Cross, Dipole, Tripole, Ring, Square Loop, and Cross Dipole—is rated from 1 (best) to 4 (least) in each category. The Square Loop shape consistently performs the best, receiving top ratings (1) in all categories, indicating its superior overall performance. In contrast, the Dipole shape excels in cross-polarization and Band Separation but scores lower in Stability and Larger Bandwidth.

Table 2. Performance of FSSs with different element shapes (based on the freestanding FSS Performance) [113].

Shape of Elements	Cross Polarization	Angular Stability	Band Separation	Larger Bandwidth
Jerusalem Cross	3	2	2	2
Dipole	1	4	1	4
Tripole	3	3	2	3
Ring	2	1	1	1
Square Loop	1	1	1	1
Cross Dipole	3	3	3	3

4. Methods for Analysis of FSS

Various techniques are employed for the numerical analysis of frequency selective surface (FSS) structures, particularly focusing on their planar and doubly periodic characteristics. The assumption that the FSS is infinite in extent allows for simplification in the analysis, where the problem can be reduced to a single unit cell. This reduction is facilitated by the application of boundary conditions that define the symmetry of the periodic, planar FSS [114]. Such simplifications are particularly effective when all elements within the unit cell are identical and the excitation is uniform across these cells, which is a common scenario in FSS analysis [115].

The analysis of FSS is typically framed within an integral equation approach that describes the behavior of the unit cell. This integral equation is modified to account for the periodic arrangement of cells, often utilizing the Floquet theorem. The theorem enables the transformation of continuous convolution integrals into infinite summations, where each term represents a product of the spectral equivalent surface and the spectral Green's function [116]. Recent advancements in numerical methods, such as the method of moments (MoM) and finite element methods (FEM), have further enhanced the efficiency of these analyses, allowing for more complex configurations and materials to be modeled accurately [115].

Moreover, the application of Floquet theory is critical in understanding the interactions within the periodic structures of FSSs. This theory provides a framework for analyzing systems with periodic coefficients, thus allowing for the exploration of various phenomena such as resonance and scattering in FSS configurations [117]. The integration of these theoretical approaches with numerical techniques has led to significant improvements in the design and optimization of FSSs for various applications, including telecommunications and radar systems [114,115].

5. FSS Measurements

Transmission and reflection are the main characteristics evaluated for an FSS, and there are only few common methods to measure them. In order to measure the transmission of an FSS, it is placed between two directive antennas, one acting as a receiver while the other acting as a transmitter. The FSS blocks the path of propagation and filters the wave radiated from the transmitter on its way to detection by the receiver antenna. The FSS plane can be rotated while the antennas are fixed for measuring the oblique incidence performance. As a reference, the power transmission between the two antennas is measured while the FSS is removed. This response is kept as a calibration, and the FSS transmission response is obtained by normalizing the measured power of the FSS to the calibration response [118].

In order to simulate a free space environment, the experiment should be performed in an echoic chamber. However, this method may not be able to measure the characteristics accurately, specifically the reflectivity. In the measurement of reflection, the undesired scattering can dominate the reflected signals. Also, the diffraction from edges of FSSs become strong and shadows the actual reflected signal because the FSS is of a finite size

and usually resides a distance from the antennas. Edge scattering also increases due to the large beamwidth of antennas [119].

5.1. Multi-Layer Frequency Selective Surfaces

Single-layer FSSs are often compact in volume and light in weight as compared to the multi-layer FSSs. Considering that in some applications of FSSs the main requirement is a wider bandwidth and higher selectivity, single-layer FSSs conventionally produce just one resonance and may not be capable of fulfilling the selectivity and bandwidth requirements [120,121]. In order to achieve a wider bandwidth and higher selectivity, multi-layer FSS structures with more complicated geometries can be used. Assembling an FSS with two identical metallic layers stacked with an impedance inverter in between produces a filter with a wider bandwidth and higher selectivity. The selectivity can be improved by implementing higher-order FSSs with additional metallic layers and impedance inverters. In addition, transmission zeros can be inserted in the out-of-band response to improve selectivity and suppress unwanted harmonics and frequency components [122,123].

However, the implementation of multi-layer FSSs can be costly and complicated compared to the single-layer structures. In addition, the numerical analysis of multi-layer structures is complicated because of the coupling effects between the fixed FSSs. Therefore, a single-layer FSS with patches and strips of different sizes can be arranged in a fractal geometry to produce multiple resonances using a single layer. This efficiently reduces the overall profile and fabrication complexity [124]. However, the fractal FSS reveals multiple unwanted resonance features because of the multiple types and size of elements per unit cell [125].

Multiband FSSs with close band spacing have been of great interest in recent research because of their application in military systems, i.e., missile, aircraft, etc. to communicate with satellites [126]. In these applications, multiple operating frequencies are used [127]. The construction of an FSS with three bands [S-band (2.2 GHz), Ku-band (14.9 GHz), and Ka-band (25.25 GHz)] is of great challenge. The reflection and transmission ratio for the center of each frequency band is 1.48 or less [128]. Consequently, to achieve closer reflection and transmission ratios, a gridded square FSS was proposed. The ratio ranges from 1.3 to 2.1 or > 2.5 for a single FSS [2], but such a design has a major drawback of fabrication complexity because of the multi-layer structures. Another way of achieving close band spacing is using the resonant frequencies of double square units with active components that have different loadings [129,130]. Subsequently, this design (dual band loaded FSS) mitigates the above-mentioned issues and achieves close band spacing, and the resonant frequency is tailored with different loadings of lumped components.

5.2. Angular Stability

As an FSS is exposed to electromagnetic radiation, it ideally acts like a filter that is independent of polarization and angle of incidence. However, in real scenarios, the electromagnetic waves might be incident with various angles and polarization. This necessitates the design of FSSs that work for all the incident angles. The reflection/transmission properties should be stable as the angle of polarization and incidence changes when the electromagnetic waves impinge the FSS. Considering an indoor environment, the signals might experience multiple reflections off walls and furniture before reaching the FSS. Figure 9 shows a unit cell consisting of a Jerusalem cross FSS alongside its reflection and transmission response. However, harmonics are present for higher ranges of incident angles.
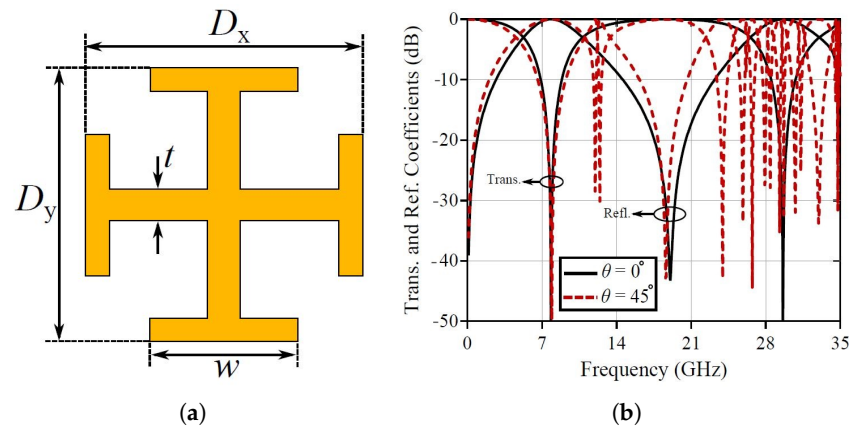
Figure 9. Frequency selective surface made of Jerusalem cross elements. (**a**) Jerusalem cross unit cell, (**b**) Simulated transmission and reflection coefficient [131].

Stable frequency response of an FSS can be achieved by selecting appropriate elements or changing FSS layers or dielectric substrates [132–134]. A double-layer configuration has been investigated for reducing the angular sensitivity [135–139]. In order to achieve higher angular stability, FSSs with unit cell sizes much smaller than the wavelength are of great interest. Such small elements avoid the excitation of higher-order brag modes and result in higher stability of the frequency response over the oblique incidences. Different methods such as using lumped elements, fractal unit cells, meandered unit cells, etc., have been utilized to miniaturize the unit cell. By reducing the electrical sizes of the constituting element to a subwavelength level and producing resonance by a combination of the miniaturized non-resonant elements, highly stable frequency responses under oblique incidence angles are achieved.

6. Pros and Cons of Traditional FSSs

Up to now, various FSS structures have been developed and introduced in the literature for a broad range of applications. Hence, the literature has shed light on the pros and cons of the FSSs, which are captured in Table 3.

Table 3. Summary of the Pros and Cons of Current FSSs [140].

	Pros	Cons
Single-Layer FSS	Simple planar	Dependent on polarization and angle of incident. Bandwidth is narrow.
Multi-layer FSS	Bandwidth is wider. Multiband	Coupling effect. Costly and difficult to construct.
Multiband responses	More Selective FSS	Fabrication process needs strict requirements. Concentric elements have unexpected coupling.
Tunable FSS	Frequency properties varies	Numerous active elements required. High cost and complex. More potential for failure.

7. 2.5-Dimensional FSSs

Miniaturized 2.5D frequency selective surfaces (FSSs) represent an innovative approach that bridges the gap between traditional two-dimensional (2D) and three-dimensional (3D) structures. These surfaces typically consist of a planar arrangement of elements with a limited vertical dimension, combining the benefits of both 2D and 3D designs. The

"2.5D" designation highlights the incorporation of a third dimension, albeit in a constrained manner, allowing for improved performance in various applications.

The 2.5-Dimensional frequency selective surfaces (FSSs) are compact and lightweight designs that integrate multi-layer configurations, allowing for functionalities such as filtering, impedance matching, and reconfigurability without increasing bulk. These surfaces often incorporate tunable elements, like MEMS switches or varactor diodes, enabling real-time adjustments to their frequency response, which is particularly beneficial in dynamic environments. Applications of 2.5D FSSs span various fields, including wearable devices, where they minimize electromagnetic interference while ensuring efficient wireless communication; smart textiles that enable advanced functionalities like environmental sensing; Internet of Things (IoT) devices that require efficient and compact communication solutions; and healthcare, where they filter noise in medical implants and wearable health-monitoring devices, thus enhancing data reliability and performance.

8. 3D Frequency Selective Structures

Recently, 3D FSSs have been proposed to overcome challenges such as slow roll-offs, sensitivity to oblique incident angles, and poor frequency selectivity faced by conventional 2D FSSs. The 3D FSS structures offer more degrees of freedom in terms of designing new geometries to achieve specifications that are challenging to realize using 2D configurations. A multimode resonator made of 2D array of cavities is proposed in [141–143]. It offers good control on the position and the numbers of transmission zeroes and poles. For instance, to achieve multiband behavior, one is required to increase the number of poles and zeroes. For traditional designs, an increase in the number of poles and zeros translates to the multi-layer FSS. The 3D FSS shows a stable angular and symmetric filtering response. The 3D FSS is stacked between two dielectric layers covered by the perfect electric conductors, and it has a wall of periodic boundary conditions as shown in Figure 10.
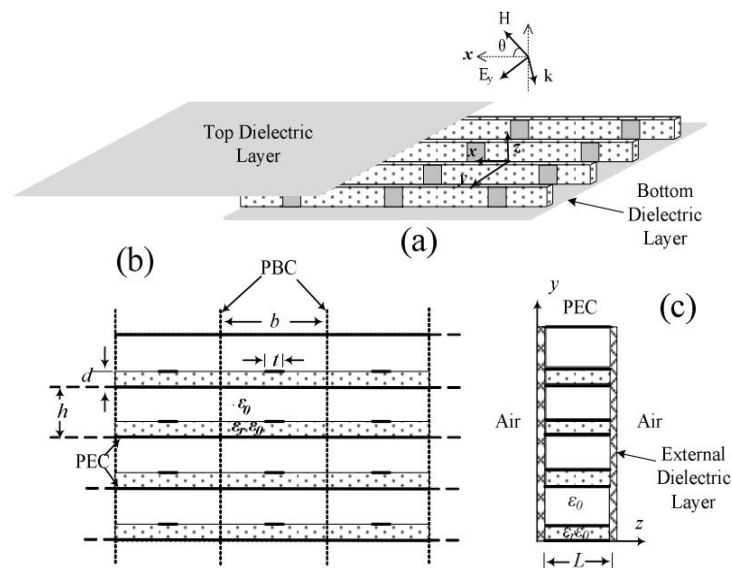

Figure 10. (**a**) Perspective view of 3D FSS; (**b**) cross-sectional view of FSS (**c**); side-view (Picture is taken from [142]).

Though 3D-FSSs have demonstrated an enhancement of filtering characteristics and more degrees of freedom, these structures are complicated to realize and fabricate. In addition, they result in thicker and bulkier profiles compared with their 2D counterparts, which is not desirable in applications requiring a light weight and thin structures. A summary of few recent 3D FSS research studies based on types of elements used, size, and operating frequency is presented in Table 4.

Table 4. Summary of recent 3D FSS investigations.

Article	Element Used	Size (mm)	Frequency (GHz)
[141]	Split microstrip lines with a thin rectangular metallic bar	10.5 × 3	5–10
[144]	U-shaped strip lines printed on a thin substrate	10 × 10	8.4–16.2
[145]	Circular ring unit cell	34 × 34	2.5–4.5
[146]	Rectangular waveguide loaded by a wire resonator	5.4 × 3	11–24
[147]	Staggered geometry of metallic rectangular frames	4.50 × 1.30	11.8–13.2
[148]	Lumped capacitor added with impedance resonator	7.5 × 3.4	4.3–4.8
[149]	3D symmetric unit cell	10 × 10	12.4–16.3
[150]	Square waveguide	9 × 7	12–24.7
[151]	Slots integrated in square waveguide	13 × 11	3.7–4
[152]	Strip lines with metallic plates	8 × 8	7–8.3

9. Miniaturized Element FSSs

As explained in Section 5.2, in order to increase the stability of the FSS response for oblique incidences of EM wave, the unit cell size must be miniaturized [111]. This is very important whenever an FSS is used in close proximity to the radiation source. To counter this problem, a new class of FSS has been developed known as miniaturized-element FSS. In this approach, non-resonant unit cells with small dimensions are used instead of fully resonant elements in traditional FSSs. When coupled to the incident electromagnetic waves, these elements behave as lumped inductors and capacitors. The combination of inductive and capacitive elements form a resonance. The electrical size of unit cells can be decreased to less than $\lambda/4$ or even less than $\lambda/10$ in some cases [153,154].

The first miniaturized-element FSS was realized by [155] as shown in Figure 11. A large array of capacitive patches is printed on one side of a thin dielectric spacer with an inductive wire grid on the other side. As the FSS is designed using miniaturized elements, its electromagnetic response can be accurately described using a lumped-element circuit model.

The equivalent circuit model of this miniaturized-element FSS is given in Figure 12a, where L inductance models the wire grid in bottom layers and C represents the capacitive patch array in the top layer. The dielectric substrate is represented by a transmission line section with $Z_l = Z_0/\sqrt{\epsilon_r}$, where $Z_0 = 377\ \Omega$ is the free space wave impedance and ϵ_r is the relative permittivity of the substrate.

Based on the circuit model in Figure 12a, the top layer array produces a passband at f_{p1} described by

$$f_r = \frac{1}{2\pi\sqrt{LC}}. \tag{6}$$

Figure 12b presents the comparison of transmission coefficients obtained from EM simulations and circuit model simulations. It is evident that a good agreement for a wide range of frequencies is achieved. The scan angle performance is displayed in Figure 13 for

both TE and TM polarization. The structure shows a reasonably stable frequency response for angles of up to 45 degree of the incident wave. Since the electromagnetic responses of the miniaturized-element FSS can be effectively modeled using lumped element circuits, a conventional circuit-based filter theory can be utilized to design the desired filtering response. Table 5 shows a summary of different miniaturized-element bandpass FSS structures with their overall thickness and fractional bandwidth.
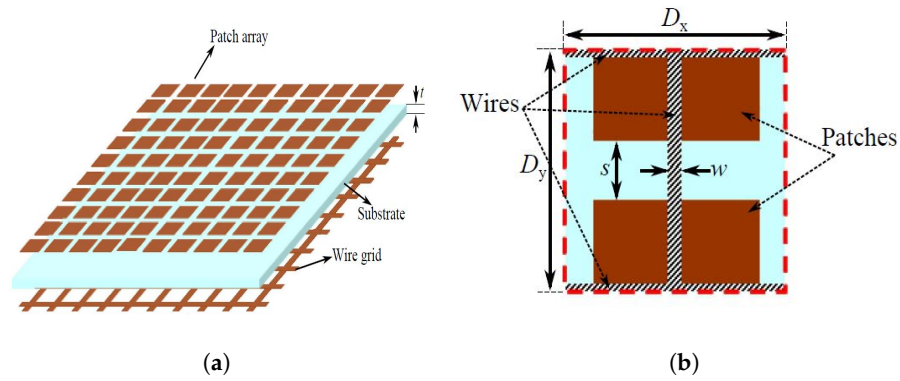

(a)   (b)

Figure 11. The first miniaturized element FSS. (**a**) 3D view of FSS, (**b**) the unit cell of the structure. (Picture taken from [112]).

(a)   (b)

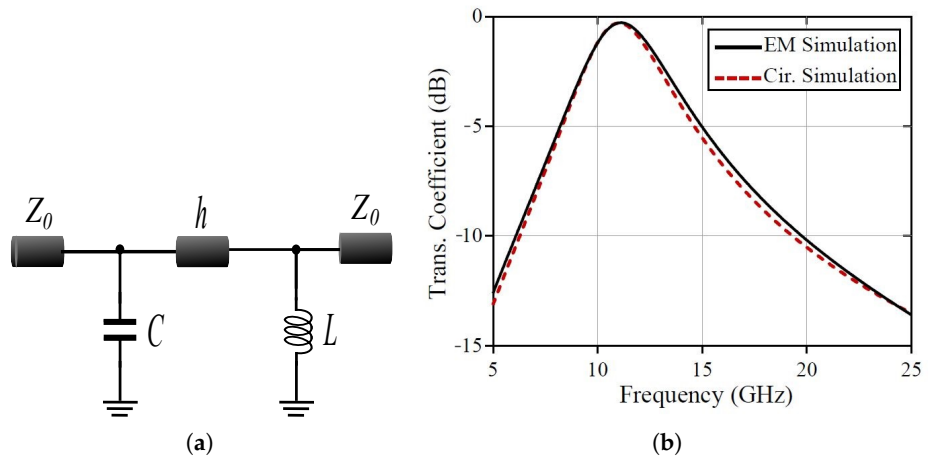**Figure 12.** (**a**) Lumped-element circuit model for miniaturized elements, (**b**) Comparison between EM and circuit model simulations with $L = 1.08$ nH and $c = 0.15$ pF (results are adopted from [112]).
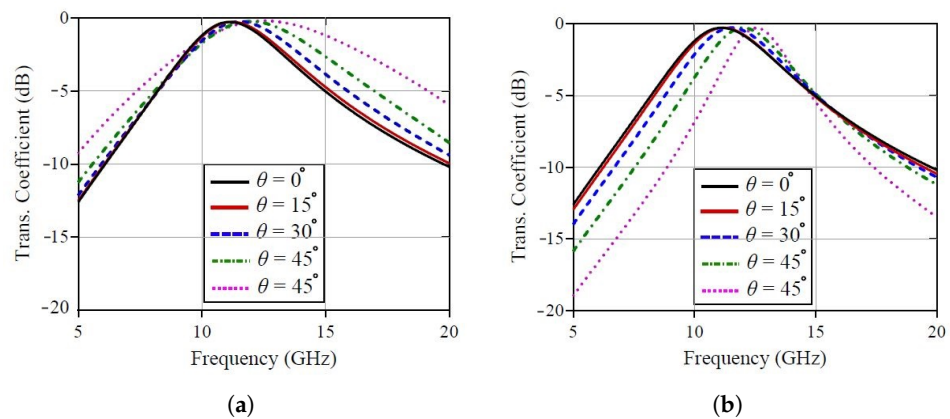

(a)   (b)

Figure 13. Scan angle performance of miniaturized-element FSS; (**a**) TE Polarization; (**b**) TM Polarization (results are adopted from [112]).

Table 5. Summary of some FSSs regarding overall thickness and fractional bandwidth.

Article	Frequency (GHz)	Thickness	Order	Bandwidth
[153]	21	$0.273\lambda_0$	second	5%
[156]	10	$0.033\lambda_0$	second	20%
[157]	10	$0.067\lambda_0$	second	21%
[158]	16.5	$0.22\lambda_0$	second	10%
[159]	8.5	$0.257\lambda_0$	third	15%

10. Switchable and Tunable FSSs

Electrically tuning the frequency response is an important feature of FSS design. For an adaptive screening of unwanted wireless transmissions, tunable FSSs are used [160,161]. Such tunable and switchable structures are usually implemented by using semiconductor device loading, i.e., PIN diodes, varactors diodes, and Schottky diodes [162–165]. DC bias is required for tuning the semiconductor devices, where the frequency response of the FSS is altered by controlling the bias voltage of the active elements. Thus, an appropriate metallic feed network should be added to the FSS to provide DC biasing to the active elements. Such a network adds to the complexity of the FSS structure and, in some cases, affects the original frequency response, especially under oblique incidences.

Another method for FSS tuning/switching is by integrating micro-electro-mechanical (MEMs) switches into the FSS unit cells, where switching the MEMs elements alters physical paths on the unit cell geometry. MEMs devices can control the FSS resonance frequency by actuating two states switched electrostatically. Switching can be performed with high speed and low DC power consumption. However, MEMs devices require a complicated fabrication process that results in high implementation cost not suitable for low-cost systems [166–168]. An overview of different types of active FSSs alongside the comparison of their fractional bandwidth and tuning range is presented in Table 6.

Table 6. An overview of types of AFSS with the comparison of their FBW and tuning range (TRs).

FSS Ref.	Type of AFSS	Switching/Tuning	FBW	Tuning	Polarization
[70]	Switchable(Passband)	PIN diodes	17		No
[169]	Tunable(Stopband)	Varactor diode	12.5	32	No
[43]	Tunable Absorber(Passband)	Varactor diode	4	5	No
[170]	Tunable(Stopband)	Varactor diode	81.4	69.5	No
[71]	Tunable	Varactor diode	152.4	129	Yes
[34]	Tunable(Stopband)	High-permittivity ceramics	25.8	22.9	No
[72]	Tunable Absorber	PIN diode	91	31.6	Yes
[33]	Tunable(Passband)	Chip capacitor	5.9	30	No
[83]	3D Tunable AFSS(Stopband)	Graphene micro-ribbons	5.5	10	No
[92]	Tunable Absorber	PIN, Varactor diode	113	47.3	No
[171]	Tunable 3D AFSS(Passband)	Varactor diode	14	65	No
[172]	Tunable(Passband)	Varactor diode	11.5	24.6	No

Other tuning methods such as liquid crystal manipulation, BST diodes, etc., have also been proposed; however, all of them suffer from high implementation complexity and biasing network requirements. In this work, tunable FSS are designed using a mechanical approach that removes the need for DC biasing. In addition, a novel embedded bias network has been used to conceive a varactor-based FSS that removes biasing interference issues and harmonic generation and minimizes lumped element or RF choke requirements.

11. Discussion

The review of frequency selective surfaces (FSSs) highlights several key findings. FSSs are planar structures composed of periodic metallic layers printed on dielectric substrates, with unit cells of varying geometrical shapes, including patches, loops, hexagons, convoluted shapes, and fractal geometries. Their frequency responses depend on these geometries and materials, categorizing them into low pass, high pass, band stop, and band pass filters. Recent research has focused on miniaturized FSSs with high selectivity, operating efficiently across multiple frequency bands. Innovations such as dual-band and multiband FSSs enhance wireless communication and mitigate electromagnetic interference. The incorporation of active components has enabled tunability and reconfigurability, with active FSSs featuring convoluted elements showing potential for dynamic control over frequency responses, paving the way for adaptive solutions in communication and sensing systems. Studies on FSSs on flexible and textile substrates suggest potential for conformal applications and cost-effective, environmentally friendly electromagnetic filters. Additionally, emerging research explores FSSs in liquid sensing and strain sensing, showcasing their adaptability for various applications beyond traditional electromagnetic uses.

The findings indicate that FSS technology is advancing rapidly, driven by the need for more efficient, compact, and adaptable electromagnetic filtering solutions. The diversity in structural designs and the ability to integrate active components reflect a trend towards more dynamic and multifunctional FSS applications. Exploring flexible and unconventional substrates suggests a shift towards practical, real-world applications where flexibility and environmental considerations are crucial. Furthermore, the innovative use of FSSs in sensing applications demonstrates their potential beyond conventional filtering roles, indicating a broader scope for future research and development.

The advancements in FSS technology have significant implications for various fields. Improved selectivity and miniaturization of FSSs can enhance the performance of wireless communication systems by providing more efficient filtering and reduced electromagnetic interference. The adaptability of FSSs for liquid and strain sensing opens new avenues for integrating these surfaces into structural engineering and environmental monitoring systems. The use of flexible and unconventional substrates for FSSs suggests potential for developing new materials and manufacturing processes, leading to cost-effective and sustainable solutions. Additionally, the application of FSSs in radomes and multiband reflector antennas demonstrates their value in defense and aerospace technologies, where efficient filtering and reduced radar cross-sections are critical.

Despite the promising advancements, there are several limitations to consider. The design and realization of FSSs with desired frequency responses require precise control over unit cell geometries and materials, which can be complex and resource-intensive. The frequency response of FSSs can degrade under oblique incidence, affecting their performance in real-world applications where waves may not always be perpendicular. Incorporating active components into FSSs for tunability and reconfigurability presents integration challenges, particularly in maintaining stability and performance. Moreover, the performance of FSSs on flexible and unconventional substrates may be limited by the mechanical and electrical properties of the materials used.

One of the key challenges in designing reconfigurable FSSs is solving optimization problems related to surface configuration. Reconfigurable FSSs must dynamically adjust their resonant frequency, polarization, and bandwidth to meet varying operational requirements. To achieve this, optimization algorithms such as genetic algorithms, particle swarm optimization, and differential evolution are commonly used. These techniques help minimize the size of the unit cell while maximizing performance across a range of frequencies.

In addition to hardware-based reconfigurations, software-defined FSS configurations offer a promising approach to improving system flexibility. In software-defined FSSs, digital controllers adjust the surface's response in real time based on the surrounding environment

and communication demands. This is particularly useful in 5G networks, where rapid frequency changes are required to manage multiple users and high data rates.

Based on the findings and implications, the following recommendations are proposed. Enhanced modeling and simulation tools should be developed to better understand the impact of unit cell geometries and materials on FSS performance, particularly under varying angles of incidence. Research should focus on integrating active components into FSSs more effectively, exploring new materials and fabrication techniques to maintain stability and performance. Interdisciplinary research should be encouraged to explore new applications of FSSs in fields such as environmental monitoring, healthcare, and smart infrastructure. Investment in developing new materials and substrates that combine flexibility, durability, and optimal electromagnetic properties is essential to expand the practical applications of FSSs. Additionally, standard testing protocols for FSS performance, particularly for flexible and unconventional substrates, should be established to ensure reliability and consistency in real-world applications.

This study underscores the continuous innovation in FSS technology, highlighting the potential for significant advancements in wireless communication, sensing, and various other applications. By addressing the limitations and focusing on the recommended areas, the development and application of FSSs can be further enhanced. The summary of the key finding is highlighted in Table 7.

Table 7. Summary of key findings in FSS research.

Key Findings	Description	Applications
Improved Design of FSS Structures	Research contributes to the development of novel FSS designs (e.g., 2.5D, miniaturized configurations) to enhance performance.	Wearable devices, IoT, healthcare devices
Electromagnetic Filtering and Interference Control	Research demonstrates how FSS can filter specific frequency bands and reduce electromagnetic interference (EMI).	Smart textiles, communication systems, radar systems
Tunable and Reconfigurable FSS	The study explored tunable FSSs using MEMS switches or varactor diodes for dynamic frequency response adaptation.	Dynamic wireless communication systems, adaptive sensors
Enhanced Bandwidth and Gain	The research shows how multi-layered and fractal-based FSS designs improve bandwidth and front-to-back gain.	5G networks, satellite communication, high-frequency antennas
Low Reflection and Return Loss	The study investigated FSS designs for low return loss and reflection in microwave and millimeter-wave applications.	Wireless communication systems, radar, medical implants
Compact and Lightweight Designs	Miniaturized designs allow FSSs to be integrated into smaller devices without compromising performance.	IoT, wearable devices, mobile communication devices

12. Conclusions

This study provides an analysis of frequency selective surfaces (FSSs), a rapidly evolving area in modern electromagnetism. Traditional FSS structures are systematically categorized into four primary groups based on their geometries: center-connected elements like dipoles and Jerusalem crosses, loop types including various legged elements and loops, solid interior or plate types, and combinations of these forms. The operational mechanisms of these traditional FSSs are fundamentally reliant on structural-based resonances, which are briefly discussed along with methods of characterization and numerical simulations.

The research presented in this paper extensively details various design techniques, array element structures, frequency ranges, bandwidths, and polarization characteristics through comparative tables. This valuable information serves as a resource for microwave researchers and the MEFSS design community, aiding in the development of new methods and facilitating comparative analysis. The study highlights the potential of FSS designs in enabling numerous practical applications across different frequency bands, including microwave, millimeter, terahertz, and optical modes.

By bridging the gap between theoretical foundations, structural parameters, and performance characteristics, this study is anticipated to advance the state-of-the-art design of FSS devices. Additionally, the research discusses innovative approaches to tuning and switching FSS, particularly the mechanical tuning method that eliminates the need for DC biasing and the novel embedded bias network designed for varactor-based FSS, which minimizes interference issues and simplifies the implementation.

Our work summarizes significant advancements in the field of frequency selective surfaces (FSSs) through several approaches. Firstly, we investigate tunable and reconfigurable FSS designs that incorporate active components, enabling dynamic control over frequency responses, which is crucial for applications in mobile communication and radar systems. Additionally, we explore the use of flexible substrates and novel geometries, such as fractal and hexagonal shapes, to enhance bandwidth and reduce beamwidth, thereby improving signal directionality. Our research also addresses fabrication challenges by proposing single-layer FSS configurations that maintain performance while simplifying manufacturing processes. Furthermore, we emphasize the importance of miniaturizing unit cell sizes to achieve higher angular stability, which is vital for applications in close proximity to radiation sources. Lastly, we highlight the potential of dual-band and multi-band FSS designs, which can effectively operate across multiple frequency bands, thus broadening their applicability in modern communication systems.

Author Contributions: Conceptualization, W.A. and W.R.; methodology, W.A.; software, W.A.; validation, W.A., M.R.R., A.E. and W.R.; formal analysis, W.A. and W.R.; investigation, W.A.; resources, M.T.A.R., M.Z.B. and W.A.; data curation, M.Z.B.; writing—original draft preparation, W.A.; writing—review and editing, A.E. and M.R.R.; visualization, M.T.A.R. and M.Z.B.; supervision, W.R. All authors have read and agreed to the published version of the manuscript.

Conflicts of Interest: The authors declare no conflicts of interest.

References

1. Li, L.; Chen, Q.; Yuan, Q.; Sawaya, K.; Maruyama, T.; Furuno, T.; Uebayashi, S. Frequency selective reflectarray using crossed-dipole elements with square loops for wireless communication applications. *IEEE Trans. Antennas Propag.* **2011**, *59*, 89–99. [CrossRef]
2. Qing, A.; Lee, C.K. Analysis of gridded square frequency selective surfaces. In Proceedings of the IEEE Asia-Pacific Microwave Conference, Sydney, Australia, 3–6 December 2000.
3. Junior, A.G.D.A.; Fontgalland, G.; Titaouine, M.; Baudrand, H.; Neto, A.G. Analysis of quasi-square open ring frequency selective surface using the Wave Concept Iterative Procedure. In Proceedings of the International Microwave and Optoelectronics Conference (IMOC), Belem, Brazil, 3–6 November 2009.
4. Jha, K.R.; Singh, G.; Jyoti, R. A simple synthesis technique of single-square loop frequency selective surface. *Prog. Electromagn. Res.* **2012**, *45*, 165–185. [CrossRef]

5. Zhang, T.; Yang, G.H.; Li, W.L.; Wu, Q. A novel double-layer semi-circle fractal multi-band frequency selective surface. In Proceedings of the International Symposium on Antennas Propagation and EM Theory (ISAPE), Guangzhou, China, 29 November–2 December 2010.

6. Sakran, F.; Neve-Oz, Y.; Ron, A.; Golosovsky, M.; Davidov, D.; Frenkel, A. Absorbing frequency-selective-surface for the mm-wave range. *IEEE Trans. Antennas Propag.* **2008**, *56*, 2649–2655. [CrossRef]

7. Zheng, S.; Yin, Y.; Ren, X. Interdigitated hexagon loop unit cells for wideband miniaturized frequency selective surfaces. In Proceedings of the IEEE, 9th International Symposium on Antennas Propagation and EM Theory (ISAPE), Guangzhou, China, 29 November–2 Decembe 2010.

8. Lu, Z.; Shen, R.; Yan, X. A novel wideband frequency selective surface composite structure. In Proceedings of the China-Japan Joint Microwave Conference Proceedings (CJMW), Hangzhou, China, 20–22 Apri 2011.

9. Brito, D.B.; Araújo, L.M.; D'Assunção, A.G.; Maniçoba, R.H. A Minkowski fractal Frequency Selective Surface with high angular stability. In Proceedings of the International Microwave and Optoelectronics Conference (IMOC), Rio de Janeiro, Brazil, 4–7 August 2013.

10. Anuradha; Patnaik, A.; Sinha, S.N.; Mosig, J.R. Design of customized fractal FSS. In Proceedings of the Antennas and Propagation Society International Symposium (APSURSI), Chicago, IL, USA, 8–14 July 2012.

11. Mathivanan, A.; Saravanan, P. Miniaturized multiband frequency selective surface with wide frequency ratio. *Microw. Opt. Technol. Lett.* **2022**, *64*, 1991–1999. [CrossRef]

12. Duarte, M. A new miniaturized active frequency selective surface with convoluted element for uhf applications. *J. Microw. Optoelectron. Electromagn. Appl.* **2024**, *23*, e2024278519 . [CrossRef]

13. Liang, Y.; Chen, M.; Peng, L. A dual-function switchable and frequency tunable active frequency selective surface. *Int. J. Microw. Comput. Aided Eng.* **2021**, *31*, e22897. [CrossRef]

14. Liu, B.; Song, K.; Xiao, J. Two-Dimensional Optical Metasurfaces: From Plasmons to Dielectrics. *Adv. Condens. Matter Phys.* **2019**, *2019*, 2329168. [CrossRef]

15. Bilal, M.; Saleem, R.; Abbasi, Q.; Kasi, B.; Shafique, M. Miniaturized and flexible fss-based em shields for conformal applications. *IEEE Trans. Electromagn. Compat.* **2020**, *62*, 1703–1710. [CrossRef]

16. Han, Y.; Feng, S.; Chen, J.; Chang, Y.; Liao, S.; Che, W. Design of paper-based bandpass frequency selective surface using slotlines. *Microw. Opt. Technol. Lett.* **2022**, *64*, 1339–1346. [CrossRef]

17. Njogu, P.; Sanz-Izquierdo, B.; Parker, E. A liquid sensor based on frequency selective surfaces. *IEEE Trans. Antennas Propag.* **2023**, *71*, 631–638. [CrossRef]

18. Soltani, S.; Taylor, P.; Parker, E.; Batchelor, J. Popup tunable frequency selective surfaces for strain sensing. *IEEE Sens. Lett.* **2020**, *4*, 1–4. [CrossRef]

19. Liang, C.; Xiao, Z.; Fan, L.; Zhou, M.; Leung, S.; Wang, Y.; Li, F.; Poo, Y. High-temperature-resistant frequency selective metasurface with low-frequency diffusion and high-frequency transmission. *J. Phys. Appl. Phys.* **2022**, *55*, 215102. [CrossRef]

20. Can, S.; Kapusuz, K.; Yılmaz, A. Optically transparent dual-band frequency selective surfaces for smart surfaces. In Proceedings of the 2022 Sixteenth International Congress on Artificial Materials for Novel Wave Phenomena (Metamaterials), Siena, Italy, 12–17 September 2022. [CrossRef]

21. Li, J. Absorption-transmission-diffusion-type radar cross section reduction metasurfaces based on frequency selective absorber and polarization conversion chessboard structure. *J. Phys. Appl. Phys.* **2024**, *57*, 225101. [CrossRef]

22. Shi, J.; Xu, B.; Tao, Z. Design of a 3-d tunable band-stop frequency selective surface with wide tuning range. *Prog. Electromagn. Res. Lett.* **2020**, *92*, 9–16. [CrossRef]

23. Huang, S.; Fan, Q.; Wang, J.; Xu, C.; Wang, B.; Yang, B.; Tian, C.; Meng, Z. Multi-spectral metasurface with high optical transparency, low infrared surface emissivity, and wideband microwave absorption. *Front. Phys.* **2020**, *8*, 385. [CrossRef]

24. Jiang, W.; Zhang, K.; Zhao, B.; Su, Y.; Gong, S. Design of miniaturised frequency selective rasorber using parallel lc resonators. *IET Microw. Antennas Propag.* **2019**, *13*, 554–558. [CrossRef]

25. Yu, Z.; Xia, Y.; Zhu, J.; Wang, C.; Shi, Y.; Tang, W. Dual-band three-dimensional fss with high selectivity and small band ratio. *Electron. Lett.* **2019**, *55*, 798–799. [CrossRef]

26. Qiu, S.; Guo, Q.; Li, Z. Tunable frequency selective surface based on a sliding 3d-printed inserted dielectric. *IEEE Access* **2021**, *9*, 19743–19748. [CrossRef]

27. Yong, W.; Glazunov, A. Miniaturization of a fully metallic bandpass frequency selective surface for millimeter-wave band applications. *IEEE Trans. Electromagn. Compat.* **2023**, *65*, 1072–1080. [CrossRef]

28. Costa, F.; Monorchio, A. A Frequency Selective Radome With Wideband Absorbing Properties. *IEEE Trans. Antennas Propag.* **2012**, *60*, 2740–2747. [CrossRef]

29. Schennum, G.H. Frequency selective surfaces for multiple frequency antennas. *Microw. J.* **1973**, *16*, 55–57.

30. Agrawal, V.D.; Imbriale, W.A. Design of a dichroic Cassegrah subrefrector. *IEEE Trans. Antennas Propag.* **1979**, *27*, 466–473. [CrossRef]

31. Wu, T.K. Four-band frequency selective surface with double-square-loop patch. *IEEE Trans. Antennas Propag.* **1994**, *42*, 1659–1663.

32. Comtesse, L.E.; Langley, R.J.; Parker, E.A.; Vardaxoglou, J.C. Frequency selective surfaces in dual and triple band offset reflector antennas. *Eur. Microw. Conf.* **1987**, *17*, 208–213.

33. Bayatpur, F.; Sarabandi, K. Tuning performance of metamaterial-based frequency selective surfaces. *IEEE Trans. Antennas Propag.* **2009**, *57*, 590–592. [CrossRef]

34. Li, L.; Wang, J.; Wang, J.; Ma, H.; Du, H.; Zhang, J.; Qu, S.; Xu, Z. Reconfigurable all-dielectric metamaterial frequency selective surface based on high-permittivity ceramics. *Sci. Rep.* **2016**, *6*, 24178. [CrossRef]

35. Bossard, J.A.; Liang, X.; Li, L.; Yun, S.; Werner, D.H.; Weiner, B.; Mayer, T.S.; Cristman, P.F.; Diaz, A.; Khoo, I.C. Tunable frequency selective surfaces and negative-zero-positive index metamaterials based on liquid crystals. *IEEE Trans. Antennas Propag.* **2008**, *56*, 1308–1320. [CrossRef]

36. Roberts, J.; Ford, K.L.; Rigelsford, J.M. Secure electromagnetic buildings using slow phase-switching frequency-selective surfaces. *IEEE Trans. Antennas Propag.* **2016**, *64*, 251–261. [CrossRef]

37. H. Li, Q.C.; Wang, Y. A Novel 2-B Multifunctional Active Frequency Selective Surface for LTE-2.1 GHz. *IEEE Trans. Antennas Propag.* **2017**, *65*, 3084–3092. [CrossRef]

38. Lee, S.W.; Fong, T.J. Electromagnetic wave scattering from an active corrugated structure. *J. Appl. Phys.* **1972**, *43*, 388–396. [CrossRef]

39. Pozar, D. Flat lens antenna concept using aperture coupled microstrip patches. *Electron. Lett.* **1996**, *32*, 2109–2111. [CrossRef]

40. Ma, H.F.; Cui, T.J. Three-dimensional broadband and broad-angle transformation-optics lens. *Nat. Commun.* **2010**, *1*, 124. [CrossRef] [PubMed]

41. Pendry, J.B. Negative refraction makes a perfect lens. *Phys. Rev. Lett.* **2000**, *85*, 3966. [CrossRef]

42. Nauman, M.; Saleem, R.; Rashid, A.K.; Shafique, M.F. A miniaturized flexible frequency selective surface for X-band applications. *IEEE Trans. Electromagn. Compat.* **2016**, *58*, 419–428. [CrossRef]

43. Yuan, H.; Zhu, B.O.; Feng, Y. A frequency and bandwidth tunable metamaterial absorber in x-band. *J. Appl. Phys.* **2015**, *117*, 173103. [CrossRef]

44. Ghebrebrhan, M.; Aranda, F.; Walsh, G.; Ziegler, D.; Giardini, S.; Carlson, J.; Kimball, B.; Steeves, D.; Xia, Z.; Yu, S.; et al. Textile Frequency Selective Surface. *IEEE Microw. Wirel. Compon. Lett.* **2017**, *27*, 989–991. [CrossRef]

45. Tennant, A.; Hurley, W.; Dias, T. Experimental knitted, textile frequency selective surfaces. *Electron. Lett.* **2012**, *48*, 1386–1388. [CrossRef]

46. Seager, R.D.; Chauraya, A.; Bowman, J.; Broughton, M.; Philpott, R.; Nimkulrat, N. Fabric based frequency selective surfaces using weaving and screen printing. *Electron. Lett.* **2013**, *49*, 1507–1509. [CrossRef]

47. Zheng, S.; Yin, Y.; Fan, J.; Yang, X.; Li, B.; Liu, W. Analysis of miniature frequency selective surfaces based on fractal antenna–filter–antenna arrays. *IEEE Antennas Wirel. Propag. Lett.* **2012**, *11*, 240–243. [CrossRef]

48. Puente, C.; Romeu, J.; Bartoleme, R.; Pous, R. Perturbation of the Sierpinski antenna to allocate operating bands. *Electron. Lett.* **1996**, *32*, 2186–2188. [CrossRef]

49. Monti, A.; Bilotti, F.; Toscano, A.; Vegni, L. Possible implementation of epsilon-near-zero metamaterials working at optical frequencies. *Opt. Commun.* **2012**, *285*, 3412–3418. [CrossRef]

50. Di Falco, A.; Zhao, Y.; Alú, A. Optical metasurfaces with robust angular response on flexible substrates. *Appl. Phys. Lett.* **2011**, *99*, 163110 . [CrossRef]

51. Saeidi, C.; van der Weide, D. Nanoparticle array based optical frequency selective surfaces: Theory and design. *Opt. Express* **2013**, *21*, 16170–16180. [CrossRef] [PubMed]

52. Li, D.; Li, T.W.; Li, E.P.; Zhang, Y.J. A 2.5-D Angularly Stable Frequency Selective Surface Using Via-Based Structure for 5G EMI Shielding. *IEEE Trans. Electromagn. Compat.* **2018**, *60*, 768–775. [CrossRef]

53. Govindaswamy, S.; East, J.; Terry, F.; Topsakal, E.; Volakis, J.L.; Haddad, G.I. Frequency-selective surface based bandpass filters in the near-infrared region. *Microw. Opt. Technol. Lett.* **2004**, *41*, 266–269. [CrossRef]

54. Smith, H.A.; Rebbert, M.; Sternberg, O. Designer infrared filters using stacked metal lattices. *Appl. Phys. Lett.* **2003**, *82*, 3605–3607. [CrossRef]

55. Bossard, J.A.; Werner, D.H.; Mayer, T.S.; Smith, J.A.; Tang, Y.U.; Drupp, R.P.; Li, L. The design and fabrication of planar multiband metallodielectric frequency selective surfaces for infrared applications. *IEEE Trans. Antennas Propag.* **2006**, *54*, 1265–1276. [CrossRef]

56. Döken, B.; Kartal, M. Easily Optimizable Dual-Band Frequency Selective Surface Design. *IEEE Antennas Wirel. Propag. Lett.* **2017**, *16*, 2979–2982. [CrossRef]

57. De Lucena Nóbrega, C.; Ribeiro da Silva, M.; da Fonseca Silva, P.H.; D'Assunção, A.G. Analysis and design of frequency selective surfaces using teragon patch elements for WLAN applications. *J. Electromagn. Waves Appl.* **2014**, *28*, 1282–1292. [CrossRef]

58. Li, H.; Yang, C.; Cao, Q.; Wang, Y. A novel active frequency selective surface with switching performance for 2.45 GHz WLAN band. *Microw. Opt. Technol. Lett.* **2016**, *58*, 1586–1590. [CrossRef]

59. Werner, D.H.; Mayer, T.S.; Baleine, C.R. Multi-Spectral Filters, Mirrors and Anti-Reflective Coatings with Subwavelength Periodic Features for Optical Devices. U.S. 12/900,967, 14 April 2011.

60. Li, B.; Shen, Z. Bandpass frequency selective structure with wideband spurious rejection. *IEEE Antennas Wirel. Propag. Lett.* **2014**, *13*, 145–148.

61. Wu, P.; Bai, F.; Xue, Q.; Liu, X.; Hui, S.R. Use of frequency-selective surface for suppressing radio-frequency interference from wireless charging pads. *IEEE Trans. Ind. Electron.* **2014**, *61*, 3969–3977. [CrossRef]

62. Yang, G.; Zhang, T.; Li, W.; Wu, Q. A novel stable miniaturized frequency selective surface. *IEEE Antennas Wirel. Propag. Lett.* **2010**, *9*, 1018–1021. [CrossRef]

63. Dewani, A.A.; O'Keefe, S.G.; Thiel, D.V.; Galehdar, A. Window RF Shielding Film Using Printed FSS. *IEEE Trans. Antennas Propag.* **2018**, *66*, 790–796. [CrossRef]

64. Kou, N.; Liu, H.; Li, L. A Transplantable Frequency Selective Metasurface for High-Order Harmonic Suppression. *Appl. Sci.* **2017**, *7*, 1240. [CrossRef]

65. Lorenzo, J.; Lázaro, A.; Villarino, R.; Girbau, D. Modulated frequency selective surfaces for wearable RFID and sensor applications. *IEEE Trans. Antennas Propag.* **2016**, *64*, 4447–4456. [CrossRef]

66. Lorenzo, J.; Lazaro, A.; Girbau, D.; Villarino, R.; Gil, E. Analysis of on-body transponders based on frequency selective surfaces. *Prog. Electromagn. Res.* **2016**, *157*, 133–143. [CrossRef]

67. Lorenzo, J.; Lazaro, A.; Villarino, R.; Girbau, D. Diversity Study of a Frequency Selective Surface Transponder for Wearable Applications. *IEEE Trans. Antennas Propag.* **2017**, *65*, 2701–2706. [CrossRef]

68. Yang, S.; Liu, P.; Yang, M.; Wang, Q.; Song, J.; Dong, L. From flexible and stretchable meta-atom to metamaterial: A wearable microwave meta-skin with tunable frequency selective and cloaking effects. *Sci. Rep.* **2016**, *6*, 21921. [CrossRef]

69. Syed, I.S.; Ranga, Y.; Matekovits, L.; Esselle, K.P.; Hay, S.G. A single-layer frequency-selective surface for ultrawideband electromagnetic shielding. *IEEE Trans. Electromagn. Compat.* **2014**, *56*, 1404–1411. [CrossRef]

70. Kiani, G.I.; Ford, K.L.; Esselle, K.P.; Weily, A.R.; Panagamuwa, C.; Batchelor, J.C. Single-layer bandpass active frequency selective surface. *Microw. Opt. Technol. Lett.* **2008**, *50*, 2149–2151. [CrossRef]

71. Ghosh, S.; Srivastava, K.V. Broadband polarization-insensitive tunable frequency selective surface for wideband shielding. *IEEE Trans. Electromagn. Compat.* **2018**, *60*, 166–172. [CrossRef]

72. Wang, H.; Kong, P.; Cheng, W.; Bao, W.; Yu, X.; Miao, L.; Jiang, J. Broadband tunability of polarization-insensitive absorber based on frequency selective surface. *Sci. Rep.* **2016**, *6*, 23081. [CrossRef] [PubMed]

73. Nguyen, T.T.; Lim, S. Wide incidence angle-insensitive metamaterial absorber for both TE and TM polarization using eight-circular-sector. *Sci. Rep.* **2017**, *7*, 3204. [CrossRef]

74. Deng, G.; Xia, T.; Fang, Y.; Yang, J.; Yin, Z. A Polarization-Dependent Frequency-Selective Metamaterial Absorber with Multiple Absorption Peaks. *Appl. Sci.* **2017**, *7*, 580. [CrossRef]

75. Liao, Z.; Gong, R.; Nie, Y.; Wang, T.; Wang, X. Absorption enhancement of fractal frequency selective surface absorbers by using microwave absorbing material based substrates. *Photonics Nanostruct.-Fundam. Appl.* **2011**, *9*, 287–294. [CrossRef]

76. Wu, G.; Hansen, V.; Gemuend, H.P.; Kreysa, E. Multi-layered Submillimeter FSS of Shifted Crossed Slot Elements for Applications in Radio Astronomy. In Proceedings of the German Microwave Conference, Ulm, Germany, 5–7 April 2005; pp. 5–7.

77. Song, K.; Mazumder, P. Design of highly selective metamaterials for sensing platforms. *IEEE Sens. J.* **2013**, *13*, 3377–3385. [CrossRef]

78. Lee, Y.; Kim, S.J.; Park, H.; Lee, B. Metamaterials and Metasurfaces for Sensor Applications. *Sensors* **2017**, *17*, 1726. [CrossRef]

79. Agahi, S.; Mittra, R. Design of a cascaded frequency selective surface as a dichroic subreflector. In Proceedings of the International Symposium on Antennas and Propagation Society, Merging Technologies for the 90's, Dallas, TX, USA, 7–11 May 1990; pp. 88–91.

80. Costa, F.; Genovesi, S.; Monorchio, A.; Manara, G. A robust differential-amplitude codification for chipless RFID. *IEEE Microw. Wirel. Compon. Lett.* **2015**, *25*, 832–834. [CrossRef]

81. Lazaro, A.; Ramos, A.; Girbau, D.; Villarino, R. A novel UWB RFID tag using active frequency selective surface. *IEEE Trans. Antennas Propag.* **2013**, *61*, 1155–1165. [CrossRef]

82. Puente Baliarda, C.; Romeu Robert, J.; Pous Andrés, R.; Garcia, X.; Benitez, F. Fractal multiband antenna based on the Sierpinski gasket. *Electron. Lett.* **1996**, *32*, 1–2. [CrossRef]

83. Wei, X.B.; Yue, G.T.; Shi, Y.; Liao, J.X.; Wang, P. Miniaturized Bandpass Filter with Mixed Electric and Magnetic Coupling Using Hexagonal Stepped Impedance Resonators. *Electromagnetics* **2013**, *33*, 550–559. [CrossRef]

84. Huang, X.; Zhang, X.; Hu, Z.; Aqeeli, M.; Alburaikan, A. Design of broadband and tunable terahertz absorbers based on graphene metasurface: Equivalent circuit model approach. *IET Microw. Antennas Propag.* **2014**, *9*, 307–312. [CrossRef]

85. Zhang, L.; Wu, Q.; Denidni, T.A. Electronically radiation pattern steerable antennas using active frequency selective surfaces. *IEEE Trans. Antennas Propag.* **2013**, *61*, 6000–6007. [CrossRef]

86. So, H.; Ando, A.; Seki, T.; Kawashima, M.; Sugiyama, T. Directional multi-band antenna employing frequency selective surfaces. *Electron. Lett.* **2013**, *49*, 243–245. [CrossRef]

87. de Oliveira, M.R.; de Melo, M.T.; Llamas-Garro, I.; Neto, A.G. Reconfigurable Cross Dipole-Hash Frequency Selective Surface. *IET Microw. Antennas Propag.* **2017**, *12*, 224–229. [CrossRef]

88. Wang, E.; Zhang, L.; Yang, G.; Gu, X. A electronically steerable radiator and reflector array antenna based on Three-Dimensional Frequency Selective Structure. In Proceedings of the 2012 5th Global Symposium on Millimeter-Waves, Harbin, China, 27–30 May 2012; pp. 119–122.

89. Li, Y.; Li, L.; Zhang, Y.; Zhao, C. Design and synthesis of multilayer frequency selective surface based on antenna-filter-antenna using Minkowski fractal structures. *IEEE Trans. Antennas Propag.* **2015**, *63*, 133–141. [CrossRef]

90. Liu, N.; Sheng, X.; Zhang, C.; Guo, D. Design of Frequency Selective Surface Structure with High Angular Stability for Radome Application. *IEEE Antennas Wirel. Propag. Lett.* **2018**, *17*, 138–141. [CrossRef]

91. Kim, P.C.; Seo, I.S.; Kim, G.H. Nanocomposite stealth radomes with frequency selective surfaces. *Compos. Struct.* **2008**, *86*, 299–305. [CrossRef]

92. Kong, P.; Yu, X.; Liu, Z.; Zhou, K.; He, Y.; Miao, L.; Jiang, J. A novel tunable frequency selective surface absorber with dual-DOF for broadband applications. *Opt. Express* **2014**, *22*, 30217–30224. [CrossRef]

93. Kim, D.; Yeo, J.; Choi, J. Compact Spatial Triple-Band-Stop Filter for Cellular/PCS/IMT-2000 Systems. *ETRI J.* **2008**, *30*, 735–737. [CrossRef]

94. Kwon, D.; Yeo, T.D.; Oh, K.S.; Yu, J.W.; Lee, W.S. Dual resonance frequency selective loop of near-field wireless charging and communications systems for portable device. *IEEE Microw. Wirel. Compon. Lett.* **2015**, *25*, 624–626. [CrossRef]

95. Wu, Q.; Zhang, S.; Zheng, B.; You, C.; Zhang, R. Intelligent Reflecting Surface-Aided Wireless Communications: A Tutorial. *IEEE Trans. Commun.* **2021**, *69*, 3313–3351. [CrossRef]

96. Basar, E.; Di Renzo, M.; De Rosny, J.; Debbah, M.; Alouini, M.S.; Zhang, R. Wireless Communications through Reconfigurable Intelligent Surfaces. *IEEE Access* **2019**, *7*, 116753–116773. [CrossRef]

97. Li, S.; Chen, J.; Wu, Q. Joint Active and Passive Beamforming for Intelligent Reflecting Surface-Assisted SWIPT Under QoS Constraints. *IEEE Commun. Lett.* **2020**, *24*, 893–897. [CrossRef]

98. Zhang, S.; Wang, W.; Xu, X. Intelligent Reflecting Surfaces for 6G Wireless Networks: Opportunities and Challenges. *IEEE Wirel. Commun.* **2021**, *28*, 38–45. [CrossRef]

99. Han, Y.; Zhang, Z.; Li, C.; Jin, S. Large Intelligent Surface-Assisted Wireless Communication Exploiting Statistical CSI. *IEEE Trans. Veh. Technol.* **2021**, *70*, 1372–1384. [CrossRef]

100. Najafi, M.; Jamali, V.; Schober, R.; Matolak, D.W. Physics-Based Modeling of Large Intelligent Reflecting Surfaces for Vehicular Communications. *IEEE Trans. Wirel. Commun.* **2021**, *20*, 3606–3621. [CrossRef]

101. Renzo, M.D.; Debbah, M.; Phan-Huy, D.T.; Zhang, R. Smart Radio Environments Empowered by Reconfigurable Intelligent Surfaces: How It Works, State of Research, and The Road Ahead. *IEEE J. Sel. Areas Commun.* **2020**, *38*, 2450–2525. [CrossRef]

102. Ding, Z.; Yan, J.; Poor, H.V. Phase-Shift Modeling and Beamforming with Reconfigurable Intelligent Surfaces: An Overview. *IEEE Signal Process. Mag.* **2020**, *37*, 141–150. [CrossRef]

103. Tang, W.; Chen, M.Z.; Zeng, S.; Zhang, R. Wireless Communications with Reconfigurable Intelligent Surface: Path Loss Modeling and Experimental Measurement. *IEEE Trans. Wirel. Commun.* **2020**, *20*, 421–439. [CrossRef]

104. Wang, P.; Zhang, Y.; Cui, T.J. Hexagonal and Fractal FSS Designs for Bandwidth and Beamwidth Optimization. *IEEE Access* **2021**, *9*, 10397–10406. [CrossRef]

105. Li, S.; Chen, J.; Wu, Q. A Novel Frequency Selective Surface for Wideband Sidelobe Suppression in High-Gain Antennas. *IEEE Trans. Antennas Propag.* **2022**, *70*, 12–23. [CrossRef]

106. Ghosh, S.; Srivastava, K.V.; Behera, A. Design and Optimization of FSS for Sidelobe Suppression in Antenna Arrays. *IEEE Trans. Electromagn. Compat.* **2021**, *63*, 730–740. [CrossRef]

107. Guo, Y.; Shen, Z. Advanced Fractal-Based FSS for High-Gain Antennas with Enhanced Bandwidth. *IEEE Antennas Propag. Mag.* **2020**, *62*, 95–103. [CrossRef]

108. Xie, Z.; Liu, Y.; Wang, Y. Multilayer FSS for Wideband Applications in Wireless Communications. *IEEE Trans. Wirel. Commun.* **2022**, *21*, 3720–3730. [CrossRef]

109. Huang, C.; Yuen, C.; Zhang, R. Frequency Selective Surfaces for 5G Applications: Enhancing Gain and Reducing Interference. *IEEE Commun. Mag.* **2020**, *58*, 144–150. [CrossRef]

110. Lv, X. Frequency-Selective Surfaces for Microwave and Terahertz Spectra. Ph.D. Thesis, The University of Adelaide, Adelaide, Australia, 2021.

111. Munk, B.A. *Frequency Selective Surfaces: Theory and Design*; Wiley: New York, NY, USA, 2000.

112. Ebrahimi, A. Metamaterial-Inspired Structures for Microwave and Terahertz Applications. Ph.D. Thesis, School of Electrical and Electronic Engineering, The University of Adelaide, Adelaide, Australia , 2016.

113. Wu, T. *Frequency Selective Surface and Grid Array*; Wiley-Interscience: Hoboken, NJ, USA, 1995; Volume 40.

114. Hu, Y.; Su, T.; Wan, T. Efficient numerical analysis of finite FSS with multilayered media by MLACA. *IET Microw. Antennas Propag.* **2019**, *13*, 1804–1810. [CrossRef]

115. Balta, S.; Kartal, M. A novel double-layer low-profile multiband frequency selective surface for 4G mobile communication system. *Appl. Comput. Electromagn. Soc.* **2022**, *37*, 420–427 [CrossRef]

116. Molero, C.; Alex-Amor, A.; Mesa, F.; Palomares-Caballero, Á.; Padilla, P. Cross-polarization control in FSSs by means of an equivalent circuit approach. *IEEE Access* **2021**, *9*, 99513–99525. [CrossRef]

117. Ganguly, S. A perspective on the relative merits/demerits of time-propagators based on Floquet theorem. *Phys. Chem. Chem. Phys.* **2023**, *25*, 29747–29773. [CrossRef] [PubMed]

118. Sabata, A.; Matekovits, L.; Buta, A.; Dassano, G.; Silaghi, A. Frequency selective surface for ultra-wide band filtering and shielding. *Sensors* **2022**, *22*, 1896. [CrossRef] [PubMed]

119. Mistry, K.; Lazaridis, P.; Zaharis, Z.; Akinsolu, M.; Liu, B.; Loh, T. Accurate antenna gain estimation using the two-antenna method. In Proceedings of the IEEE Conference Publications, Birmingham, UK, 11–12 November 2019; 4p. [CrossRef]

120. Qin, T.; Huang, C.; Cai, Y.; Lin, X. Dual-band frequency selective surface with different polarization selectivity for wireless communication application. *Sensors* **2023**, *23*, 4264. [CrossRef] [PubMed]

121. Yan, X.; Kong, X.; Wang, Q.; Xing, L.; Feng, X.; Xu, Y.; Jiang, S. Water-based reconfigurable frequency selective rasorber with thermally tunable absorption band. *IEEE Trans. Antennas Propag.* **2020**, *68*, 6162–6171. [CrossRef]
122. Urul, B.; Tütüncü, B.; Helhel, S. A fast and novel method for determining working volume in the reverberation chamber: Position of TX antenna affect. *Microw. Opt. Technol. Lett.* **2019**, *62*, 244–250. [CrossRef]
123. Yang, X.; Wang, L.; Shen, X.; Liu, X.; Qi, T.; Zhou, Y. Single-substrate double-side high selectivity frequency selective surface. *Prog. Electromagn. Res. Lett.* **2020**, *92*, 85–92. [CrossRef]
124. Chomtong, P.; Krachodnok, P.; Bandudej, K.; Akkaraekthalin, P. A multiband FSS director using aperture interdigital structure for wireless communication systems. *IEEE Access* **2022**, *10*, 11206–11219. [CrossRef]
125. Boursianis, A.; Papadopoulou, M.; Nikolaidis, S.; Sarigiannidis, P.; Psannis, K.; Georgiadis, A.; Tentzeris, M.; Goudos, S. Novel design framework for dual-band frequency selective surfaces using multi-variant differential evolution. *Mathematics* **2021**, *9*, 2381. [CrossRef]
126. Abdollahvand, M.; Martinez-de-Rioja, E.; Forooraghi, K.; Atlasbaf, Z.; Encinar, J.; Ghosh, S.; Ebrahimi, A. Active frequency selective surface with switchable response for satellite communications in X and Ka bands. *Int. J. Microw. Comput. Aided Eng.* **2022**, *32*, e23255. [CrossRef]
127. Sen, G.; Das, S. A bi-directional dual-bandwidth microwave absorber for applications in X and Ku bands. *Int. J. Microw. Wirel. Technol.* **2019**, *11*, 983–987. [CrossRef]
128. Fan, Y.; Lin, X.; Yang, X. An FSS-based shared-aperture antenna for 5G/Wi-Fi communication and indoor 5G blind compensation. *Int. J. Microw. Wirel. Technol.* **2022**, *15*, 1373–1381. [CrossRef]
129. Govindan, T.; Palaniswamy, S.; Kanagasabai, M.; Kumar, S.; Alsath, G. Low specific absorption rate quad-port multiple-input-multiple-output limber antenna integrated with flexible frequency selective surface for WBAN applications. *Flex. Print. Electron.* **2023**, *8*, 015018. [CrossRef]
130. Wang, S.; Zheng, L.; Yan, M.; Wang, J.; Qu, S.; Luo, R. Design and analysis of miniaturized low profile and second-order multi-band polarization selective surface for multipath communication application. *IEEE Access* **2019**, *7*, 13455–13467. [CrossRef]
131. Baena, J.D.; Jelinek, L.; Marques, R.; Mock, J.J.; Gollub, J.; Smith, D.R. Isotropic frequency selective surfaces made of cubic resonators. *Appl. Phys. Lett.* **2007**, *91*, 191105. [CrossRef]
132. Bayatpur, F.; Sarabandi, K. Miniaturized FSS and patch antenna array coupling for angle-independent, high-order spatial filtering. *IEEE Microw. Wirel. Compon. Lett.* **2010**, *20*, 79–81. [CrossRef]
133. Ranga, Y.; Matekovits, L.; Esselle, K.P.; Weily, A.R. Oblique incidence performance of UWB frequency selective surfaces for reflector applications. In Proceedings of the IEEE International Symposium on Antennas and Propagation (APSURSI), Spokane, WA, USA, 3–8 July 2011.
134. Ma, T.; Zhou, H.; Yang, Y.; Liu, B. A FSS with stable performance under large incident angles. *Prog. Electromagn. Res. Lett.* **2013**, *41*, 159–166. [CrossRef]
135. Zhou, H.; Qu, S.; Xu, Z.; Wang, J.; Ma, H.; Peng, W.; Lin, B.; Bai, P. A triband second-order frequency selective surface. *IEEE Antennas Wirel. Propag. Lett.* **2011**, *10*, 507–509. [CrossRef]
136. Luo, G.Q.; Hong, W.; Lai, Q.H.; Wu, K.; Sun, L.L. Design and Experimental Verification of Compact Frequency-Selective Surface With Quasi-Elliptic Bandpass Response. *IEEE Trans. Microw. Theory Tech.* **2007**, *55*, 2481–2487. [CrossRef]
137. Lin, L.; Roberts, A. Angle-robust resonances in cross-shaped aperture arrays. *Appl. Phys. Lett.* **2010**, *97*, 061109. [CrossRef]
138. Hosseini, M.; Pirhadi, A.; Hakkak, M. A novel AMC with little sensitivity to the angle of incidence using 2-layer jerusalem cross FSS. *Prog. Electromagn. Res.* **2006**, *64*, 43–51. [CrossRef]
139. Yan, M.; Qu, S.; Wang, J.; Zhang, J.; Zhang, A.; Xia, S.; Wang, W. A novel miniaturized frequency selective surface with stable resonance. *IEEE Antennas Wirel. Propag. Lett.* **2014**, *13*, 639–641. [CrossRef]
140. Azemi, S.N. 3-D Frequency Selective Structures. Ph.D. Thesis, RMIT University, Melbourne, Australia , 2015.
141. Li, B.; Shen, Z. Three-dimensional bandpass frequency-selective structures with multiple transmission zeros. *IEEE Trans. Microw. Theory Tech.* **2013**, *61*, 3578–3589. [CrossRef]
142. Rashid, A.K.; Shen, Z. Three-dimensional monolithic frequency selective structure with dielectric loading. In Proceedings of the Asia-Pacific in Microwave Conference Proceedings (APMC), Yokohama, Japan, 7–10 December 2010.
143. Afzal, W. Highly Selective Miniaturised-Element Frequency Selective Surfaces with Tuning Capabilities. Ph.D. Thesis, RMIT University, Melbourne, Australia, 2022.
144. Rashid, A.K.; Li, B.; Shen, Z. An overview of three-dimensional frequency-selective structures. *IEEE Antennas Propag. Mag.* **2014**, *56*, 43–67. [CrossRef]
145. Azemi, S.N.; Ghorbani, K.; Rowe, W. 3D frequency selective surfaces. *Prog. Electromagn. Res.* **2012**, *29*, 191–203. [CrossRef]
146. Bihan, P.L.; García-Vigueras, M.; Fourn, E.; Gillard, R.; Naneix, I.L.R.; Varault, S.; Renard, C. Three-Dimensional Frequency Selective Surface for Single-Polarized Filtering Applications with Angular Stability. In Proceedings of the 2020 14th European Conference on Antennas and Propagation (EuCAP), Copenhagen, Denmark, 15–20 March 2020; pp. 1–4. [CrossRef]
147. Liang, B.; Bai, M. Subwavelength three-dimensional frequency selective surface based on surface wave tunneling. *Opt. Express* **2016**, *24*, 14697–14702. [CrossRef]
148. Li, B.; Shen, Z. Miniaturized bandstop frequency-selective structure using stepped-impedance resonators. *IEEE Antennas Wirel. Propag. Lett.* **2012**, *11*, 1112–1115. [CrossRef]

149. Huang, X.J.; Yang, C.; Lu, Z.H.; Liu, P.G. A Novel Frequency Selective Structure with Quasi-Elliptic Bandpass Response. *IEEE Antennas Wirel. Propag. Lett.* **2012**, *11*, 1497–1500. [CrossRef]

150. Pelletti, C.; Mittra, R.; Bianconi, G. Three-dimensional FSS elements with wide frequency and angular response. In Proceedings of the 2013 International Symposium on Electromagnetic Theory, Hiroshima, Japan, 20–24 May 2013; pp. 698–700.

151. Wang, C.; Zhuang, W.; Tang, W. Novel three-dimensional frequency selective surface with incident angle and polarization independence. In Proceedings of the 2015 International Symposium on Antennas and Propagation (ISAP), Hobart, Australia, 9–12 November 2015; pp. 1–3.

152. Li, B.; Shen, Z. Three-dimensional dual-polarized frequency selective structure with wide out-of-band rejection. *IEEE Trans. Antennas Propag.* **2014**, *62*, 130–137. [CrossRef]

153. Momeni Hasan Abadi, S.; Behdad, N. Inductively-Coupled Miniaturized-Element Frequency Selective Surfaces With Narrowband, High-Order Bandpass Responses. *IEEE Trans. Antennas Propag.* **2015**, *63*, 4766–4774. [CrossRef]

154. Afzal, W.; Ebrahimi, A.; Robel, M.R.; Rowe, W.S.T. Low-Profile Higher-Order Narrowband Bandpass Miniaturized-Element Frequency-Selective Surface. *IEEE Trans. Antennas Propag.* **2023**, *71*, 3736–3740. [CrossRef]

155. Sarabandi, K.; Behdad, N. A Frequency Selective Surface with Miniaturized Elements. *IEEE Trans. Antennas Propag.* **2007**, *55*, 1239–1245. [CrossRef]

156. Al-Joumayly, M.; Behdad, N. A New Technique for Design of Low-Profile, Second-Order, Bandpass Frequency Selective Surfaces. *IEEE Trans. Antennas Propag.* **2009**, *57*, 452–459. [CrossRef]

157. Yan, M.; Qu, S.; Wang, J.; Zhang, A.; Zheng, L.; Pang, Y.; Zhou, H. A Miniaturized Dual-Band FSS With Second-Order Response and Large Band Separation. *IEEE Antennas Wirel. Propag. Lett.* **2015**, *14*, 1602–1605. [CrossRef]

158. Gao, M.; Momeni Hasan Abadi, S.M.A.; Behdad, N. A Dual-Band, Inductively Coupled Miniaturized-Element Frequency Selective Surface With Higher Order Bandpass Response. *IEEE Trans. Antennas Propag.* **2016**, *64*, 3729–3734. [CrossRef]

159. Gao, M.; Abadi, S.M.A.M.H.; Behdad, N. A Hybrid Miniaturized-Element Frequency Selective Surface With a Third-Order Bandpass Response. *IEEE Antennas Wirel. Propag. Lett.* **2017**, *16*, 708–711. [CrossRef]

160. d'Elia, U.; Pelosi, G.; Pichot, C.; Selleri, S.; Zoppi, M. A physical optics approach to the analysis of large frequency selective radomes. *Prog. Electromagn. Res.* **2013**, *138*, 537–553. [CrossRef]

161. Niroo-Jazi, M.; Denidni, T. Reconfigurable dual-band frequency selective surfaces using a new hybrid element. In Proceedings of the 2011 IEEE International Symposium on Antennas and Propagation (APSURSI), Spokane, WA, USA, 3–8 July 2011.

162. Munir, A.; Fusco, V.; Malyuskin, O. Tunable frequency selective surfaces characterisation. In Proceedings of the 38th European Microwave Conference, Amsterdam, The Netherlands, 27–31 October 2008; pp. 813–816.

163. Amjadi, S.M.; Soleimani, M. Design of band-pass waveguide filter using frequency selective surfaces loaded with surface mount capacitors based on split-field update FDTD method. *Prog. Electromagn. Res.* **2008**, *1*, 271–281. [CrossRef]

164. Mias, C. Varactor-tunable frequency selective surface with resistive-lumpedelement biasing grids. *IEEE Microw. Wirel. Compon. Lett.* **2005**, *15*, 570–572. [CrossRef]

165. Ucar, M.H.; Sondas, A.; Erdemli, Y.E. Switchable split-ring frequency selective surfaces. *Prog. Electromagn. Res.* **2008**, *6*, 65–79. [CrossRef]

166. Bossard, J.A.; Werner, D.H.; Mayer, T.S.; Drupp, R.P. A novel design methodology for reconfigurable frequency selective surfaces using genetic algorithms. *IEEE Trans. Antennas Propag.* **2005**, *53*, 1390–1400. [CrossRef]

167. Zendejas, J.M.; Gianvittorio, J.P.; Rahmat-Samii, Y.; Judy, J.W. Magnetic MEMS reconfigurable frequency-selective surfaces. *J. Microelectromech. Syst.* **2006**, *15*, 613–623. [CrossRef]

168. Afzal, W.; Ebrahimi, A.; Robel, M.R.; Rowe, W.S. Mechanistically Independent Tunable Dual Band FSS. In Proceedings of the IEEE International Symposium on Antennas and Propagation and INC/USNC-URSI Radio Science Meeting (AP-S/INC-USNC-URSI), Firenze, Italy, 14–19 July 2024; pp. 1829–1830. [CrossRef]

169. Withayachumnankul, W.; Fumeaux, C.; Abbott, D. Planar Array of Electric- LC Resonators With Broadband Tunability. *IEEE Antennas Wirel. Propag. Lett.* **2011**, *10*, 577–580. [CrossRef]

170. Sanz-Izquierdo, B.; Parker, E.A.; Robertson, J.B.; Batchelor, J.C. Tuning patch-form FSS. *Electron. Lett.* **2010**, *46*, 329–330. [CrossRef]

171. Huang, X.G.; Shen, Z.; Feng, Q.Y.; Li, B. Tunable 3D bandpass frequency-selective structure with wide tuning range. *IEEE Trans. Antennas Propag.* **2015**, *63*, 3297–3301. [CrossRef]

172. Lin, B.Q.; Qu, S.B.; Tong, C.M.; Zhou, H.; Zhang, H.Y.; Li, W. Varactor-tunable frequency selective surface with an embedded bias network. *Chin. Phys.* **2013**, *22*, 094103. [CrossRef]